Agricultural and Forest Meteorology 276-277 (2019) 107609

Contents lists available at ScienceDirect

Agricultural and Forest Meteorology

journal homepage: www.elsevier.com/locate/agrformet

Review

Assimilation of remote sensing into crop growth models: Current status and perspectives

Jianxi Huang[a,b,c,d,*], Jose L. Gómez-Dans[e,f], Hai Huang[a], Hongyuan Ma[f], Qingling Wu[f], Philip E. Lewis[e,f], Shunlin Liang[g,h], Zhongxin Chen[i], Jing-Hao Xue[j], Yantong Wu[k], Feng Zhao[l], Jing Wang[m], Xianhong Xie[n]

[a] College of Land Science and Technology, China Agricultural University, Beijing 100083, China
[b] Key Laboratory of Remote Sensing for Agri-Hazards, Ministry of Agriculture and Rular Affairs, Beijing 100083, China
[c] Key Laboratory of Agricultural Land Quality and Monitoring, Ministry of Natural Resources, Beijing 100083, China
[d] China Meteorological Administration•Henan Key Laboratory of Agrometeorological Support and Applied Technique, Zhengzhou, 450003, China
[e] National Centre for Earth Observation (NCEO), UK
[f] Department of Geography, University College London, London, WC1E 6BT, UK
[g] Department of Geographical Sciences, University of Maryland, College Park MD 20742, USA
[h] Wuhan University, School of Remote Sensing and Information Engineering, Wuhan 430072, Hubei, China
[i] Institute of Agricultural Resources and Regional Planning, Chinese Academy of Agricultural Sciences,Beijing, 100081, China
[j] Department of Statistical Science, University College London, London, WC1E 6BT, UK
[k] School of Resources and Environment, University of Electronic Science and Technology of China,Chengdu, 611731, China
[l] School of Instrumentation and Optoelectronic Engineering, Beihang University, Beijing, 100083, China
[m] College of Resources and Environmental Sciences, China Agricultural University, Beijing, 100083, China
[n] State Key Laboratory of Remote Sensing Science, Institute of Remote Sensing Science and Engineering, Faculty of Geographical Science, Beijing Normal University, Beijing, 100875, China

ARTICLE INFO

Keywords:
Remote sensing
Crop growth models
Data assimilation
Crop modelling
Crop yield prediction
Crop monitoring

ABSTRACT

Timely monitoring of crop lands is important in order to make agricultural activities more sustainable, as well as ensuring food security. The use of Earth Observation (EO) data allows crop monitoring at a range of spatial scales, but can be hampered by limitations in the data. Crop growth modelling, on the other hand, can be used to simulate the physiological processes that result in crop development. Data assimilation (DA) provides a way of blending the monitoring properties of EO data with the predictive and explanatory abilities of crop growth models. In this paper, we first provide a critique of both the advantages and disadvantages of both EO data and crop growth models. We use this to introduce a solid and robust framework for DA, where different DA methods are shown to be derived from taking different assumptions in solving for the *a posteriori* probability density function (pdf) using Bayes' rule. This treatment allows us to provide some recommendation on the choice of DA method for particular applications. We comment on current computational challenges in scaling DA applications to large spatial scales. Future areas of research are sketched, with an emphasis on DA as an enabler for blending different observations, as well as facilitating different approaches to crop growth models. We have illustrated this review with a large number of examples from the literature.

1. Introduction

Monitoring and forecast local crop production are critical steps in addressing food security problems at a global scale. The combined effects of a changing climate, growing population, soil loss, as well as the natural variability of weather, require methods that provide a timely and accurate assessment of crop growth and production, and contribute towards increasing sustainability of agricultural food production (FAO, 2017; IPCC, 2018).

Remote sensing (RS) data have the potential to provide timely, ubiquitous and frequent observations of the land surface at a range of spatial scales (Liang and Qin, 2008). Different sensors acquire data in different spectral windows using different sensing modes: In the solar reflective domain, radiation from the sun is scattered by the atmosphere

* Corresponding author at: College of Land Science and Technology, China Agricultural University, No. 17 Qinghua East Road, Haidian District, Beijing 100083, China.
E-mail address: jxhuang@cau.edu.cn (J. Huang).

https://doi.org/10.1016/j.agrformet.2019.06.008
Received 1 December 2018; Received in revised form 26 May 2019; Accepted 5 June 2019

and land surface (soil, vegetation, etc.) and then captured by a sensor; in the (active) microwave domain, a sensor irradiates the land surface and records the echoes. In either case, these recorded observations require interpretation to provide inferences on biophysical parameters of interest for monitoring the land surface (and in particular, croplands), such as soil moisture (SM) (Njoku et al., 2003; Kerr et al., 2010; Liu et al., 2012; Dorigo et al., 2017), leaf area index (LAI) (Knyazikhin et al., 1998; Yang et al., 2006; Tian et al., 2002a,b), evapotranspiration (ET) (Mu et al., 2007), the fraction of absorbed photosynthetically active radiation (FAPAR) (Knyazikhin et al., 1998), or above ground biomass (AGB) (Hu et al., 2016).

Simultaneously, there have been significant advances in modelling crop growth and development using mechanistic models (Williams et al., 1989; Van Diepen et al., 1989; Jones et al., 2003; Challinor et al., 2004; Hsiao et al., 2009; Holzworth et al., 2015). These models predict the evolution of the crop from sowing to harvest by simulating photosynthesis, gas exchanges between the canopy and the atmosphere, phenology, soil moisture and temperature dynamics, biomass growth and grain yield formation. These models require meteorological inputs, such as downwelling shortwave radiation, temperature, precipitation, etc. (Hoogenboom, 2000). In addition to these drivers, parameters describing the different processes, crop varieties, soil conditions, management practices, etc., are also required. The models thus allow quantitative predictions of crop evolution in terms of different aspects (leaf area, above ground biomass, root biomass, soil moisture, grain yield, etc.). Although the performance of models is acceptable on its own, it is important to understand that their performance is hampered by uncertainty in the model parameterisation, uncertainty in meteorological drivers, and uncertainty in the simplified description of the model processes itself (Dorigo et al., 2007; Marin et al., 2017).

Both of the approaches described above, earth observations (EO) and crop growth models (CGM), have marked advantages, but also important disadvantages. Optical EO data can suffer from significant gaps in the data record due to e.g. cloud cover (Wiseman et al., 2014; Whitcraft et al., 2015). Additionally, retrieved parameters can have large (often unknown) uncertainties and important and not well-characterised biases (Lewis et al., 2012; Huang et al., 2015b, 2016). Additionally, EO sensors only measure a limited set of variables of interest. Crop growth models on the other hand can be difficult to parameterise properly for large scale (e.g. regional) applications, as the intrinsic variability of agriculture (different crop varieties, variations in soil types, different crop management practices) can vary hugely. Additionally, uncertainty from e.g. interpolated weather station data used as an input to the model can substantially hamper the ability of the crop model to predict crop evolution (Hansen and Jones, 2000).

It is desirable to combine crop growth models and observations, so as to exploit the best of both realms. Data assimilation (DA) techniques allow a formal and well-understood way to combine the predictions of the model with observations to arrive at an "analysis" that is an optimal combination of both inputs: the model is made to track observations, hence limiting drift due to poor local parameterisation, and the observations might also be impacted by the crop growth model providing an expectation of parameters that can be exploited for parameter retrieval.

Different from previous data assimilation reviews (Maas, 1988; Delécolle et al., 1992; Liang, 2004; Dorigo et al., 2007; Lewis et al., 2012; Kasampalis et al., 2018; Jin et al., 2018), this review focuses on the techniques in DA and explaining what approach should be used in which circumstances and why. It provides a common Bayesian framework for the different data assimilation methods presented in the literature, with a view to provide users with selection criteria to choose among them. In addition, this review summarises challenges of improving the performance of data assimilation for agricultural applications. Finally, the future development and perspective of RS-crop model data assimilation research are also discussed.

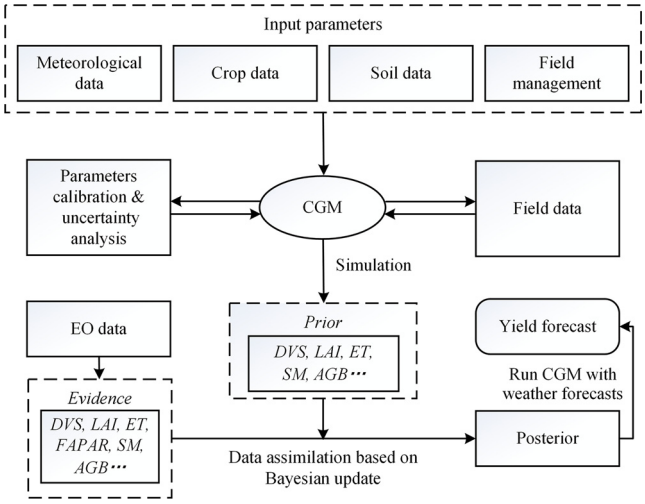

Fig. 1. Schematic representation of a typical DA system.

2. Data assimilation system illustration

Data assimilation was first proposed by Charney et al. (1969). Since then, it was gradually applied to atmospheric circulation models, such as numerical weather prediction (Dee et al., 2011), ocean circulation models (Carton and Giese, 2008), and land surface models (Yang et al., 2007). In DA, either the state of the system (e.g. the parameters that describe the system at a given point and location), the model parameters (often assumed to be constant throughout the time of the model run), or the initial conditions of some processes are assumed to be random variables, defined with a probability density function (pdf). The shape of the pdf critically encodes the uncertainty in our belief in the value of the parameters or state. DA methods provide a way to phrase the combination of observations (e.g. evidence) and models in an optimal way, by generally using Bayes' rule to update a prior pdf (e.g. predictions from a crop growth model) when evidence (e.g. uncertain EO data-derived parameters) is available. A number of different methods have been developed to do this Bayesian update, their relative merits are usually based on the assumptions made to solve for the *a posteriori* (analysis) parameter/state pdf.

Fig. 1 depicts a typical DA system. A crop growth model, e.g., WOFOST (WOrld FOod STudies), will be used as a *dynamic model*. A first step consists of collecting field data to localise or calibrate the model for a particular region. As the model not only is an approximation to real processes, but also has a considerable number of parameters that are hard to measure accurately or even at all, an initial calibration will attempt to provide a parameterisation or calibration of the model that aims to be consistent with the spatially limited field measurements (and their uncertainty). The calibrated model will then be able to forecast crop growth and development. If uncertainties in the calibrated parameters have been calculated, these can be propagated through the model to account for limitations in the calibration process.

After calibration, the model is localised and ready to use. Running the model will provide predictions of a large number of parameters, such as leaf area index (LAI), soil moisture (SM), evapotranspiration (ET), above ground biomass (AGB) and development state (DVS). EO has the potential to provide independent estimates of these quantities over large areas. DA methods will seek to update the uncertain model predictions of LAI, SM, etc. to match the uncertain observations, so that the analysis state/parameter probability density function (pdf) is consistent with both the model and observations, and providing a correction to the evolution of the model calibrated with a limited field scale dataset. The availability of short-term as well as seasonal forecasts can be used to run the model forward towards harvest and to produce predictions of e.g. crop yield.

3. Data assimilation methods

3.1. Basic theoretical background

It is instructive to consider a generic framework for data assimilation, and use that framework to explore the different approaches taken in the literature to perform model and observations combinations.

In the DA literature, we use the term state vector to denote the set of parameters that describe the condition of the crop at any given time. These parameters can include the amount of leaf area, phenological stage, amount of biomass in different organs, etc.. The task of DA is to infer the state vector given a set of (incomplete) observations. We can assume further that instead of being interested in the state vector, we are interested in its pdf. The shape of the pdf defines our belief in the values of the parameters, and is thus a measure of our uncertainty in the parameters. Once this is established, Bayes' rule is a convenient way to proceed to derive different DA approaches.

From Bayes' rule (Lee, 2012; Gelman et al., 2013), we have that the *a posteriori* pdf $p(\vec{x}|\vec{y})$ of the state vector $\vec{x}$ conditioned on the observations $\vec{y}$ is given by

$$p(\vec{x}|\vec{y}) = \frac{p(\vec{x})\cdot p(\vec{y}|\vec{x})}{p(\vec{y})} \propto p(\vec{x})\cdot p(\vec{y}|\vec{x}), \tag{1}$$

where $p(\vec{x})$ is the *a priori* pdf and $p(\vec{y}|\vec{x})$ is the *likelihood function*. The product of these two provides us with the posterior pdf $p(\vec{x}|\vec{y})$, as $\vec{y}$ are fixed observations during the Bayesian inference. That is, it is the likelihood function that brings the evidence (EO data) into the system.

As a first approximation, let us only consider the likelihood function. Under the commonly made assumption of additive Gaussian uncertainty (with mean zero and covariance matrix $\mathbf{C}_{obs}$) in the observations, and using $M(\vec{x})$ to denote the crop growth model producing predictions of the same parameters present in the observations $\vec{y}$, we have that

$$M(\vec{x}) = \vec{y} + \mathcal{N}(0, \mathbf{C}_{\text{obs}}). \tag{2}$$

In other words, if the true state $\vec{x}$ is known, the model will produce a prediction that is identical to the observations, except for the uncertainty in the latter. We assume here that the crop growth model is perfect (i.e. it has no error).

It is convenient to use the logarithm of the likelihood function, $\log p(\vec{y}|\vec{x})$ instead of the function itself: the logarithm is a monotonically increasing transform of the original function, so the location of extrema will be the same. Additionally, logarithms simplify products into sums, which results in numerical stability when implemented in digital computers with finite precision arithmetic. In our case, the log-likelihood function can be written as

$$\log p(\vec{y}|\vec{x}) = -\frac{1}{2}[M(\vec{x}) - \vec{y}]^{\top}\mathbf{C}_{\text{obs}}^{-1}[M(\vec{x}) - \vec{y}] + \text{Const.} \tag{3}$$

From Eq. (3), the most likely solution is the one attaining the maximum of $\log p(\vec{y}|\vec{x})$, which is equivalent to minimising the mismatch between the model predictions and the observations, modulated by the associated uncertainties in the observations.

There are situations where the observations are not directly relatable to the model predictions. This happens when for example surface reflectance or backscatter is assimilated directly, instead of products derived from these original measurements (Huang et al., 2019; Ma et al., 2008; Thorp et al., 2012; Wu et al., 2013; Zhou et al., 2017). In that case, the use of an *observation operator* $H(M(\vec{x}))$, such as empirical relationships or physical models of radiative transfer (RT) models, allows one to map from predicted state variables to the observations so that a comparison can be made.

The uncertainty in the estimated parameters from minimising the negative log-likelihood can be calculated by exploring the radius of the curvature of the function around the minimum using the Hessian, the matrix of second order derivatives.

So far, we have ignored the use of the prior. An important observation on the minimisation of functionals like that introduced in Eq. (3) is that due to the uncertainty in observations and model, the limited number of observations, the limited sensitivity of observations to some part of the state vector and the large number of parameters in the state vector that have an impact on the predictions of the model, it is often the case that the system is *ill posed*: a large number of parametrisations of $\vec{x}$ will result in acceptable predictions of the observations. The role of the prior is to act as extra constraint on the inference, limiting the solution space. There are a number of ways in which prior information can be introduced into these systems. A first approach would be to provide a prior pdf of $\vec{x}$ based on e.g. previous studies or expert opinions. The family of the prior pdf is subjective, and ought to reflect the understanding of the parameters. Once the prior pdf is selected, and the likelihood is similarly defined, the Bayesian update equation (Eq. (1)) can be used to find the *a posteriori* pdf of the state vector.

If we make some further assumptions on the prior pdf, such as it being a multivariate normal distribution $\mathcal{N}(\vec{\mu}, \mathbf{C}_{\text{prior}})$, it follows that the negative log-posterior is given by

$$\begin{aligned} -\log p(\vec{x}|\vec{y}) &= J_{\text{obs}}(\vec{x}) + J_{\text{prior}}(\vec{x}) + \text{Const} \\ &= \frac{1}{2}[H(M(\vec{x})) - \vec{y}]^{\top}\mathbf{C}_{\text{obs}}^{-1}[H(M(\vec{x})) - \vec{y}] \\ &\quad + \frac{1}{2}[\vec{x} - \vec{\mu}]^{\top}\mathbf{C}_{\text{prior}}^{-1}[\vec{x} - \vec{\mu}] + \text{Const.} \end{aligned} \tag{4}$$

In Eq. (4), if the dynamic model and the observation operator are linear (or not excessively non-linear), there is an analytic solution for the posterior: it is Gaussian, with a mean vector given by the minimum of cost function $J(\vec{x}) = J_{\text{obs}}(\vec{x}) + J_{\text{prior}}(\vec{x})$, and a covariance matrix derived from the inverse of the Hessian of $J(\vec{x})$ evaluated at the minimum. That is, in the case of linear dynamic model and linear observation operator, analytic expressions for both mean vector and covariance matrix are directly available. For non-linear mappings, the solution can be approximated as a Gaussian pdf by minimising the combined cost function using a non-linear solver to provide the mean, and evaluating the Hessian at the minimum to indicate the covariance.

A further observation derived from Bayes' rule is that the posterior pdf at one time step t can be thought of as the prior pdf for a (yet unobserved) observation at time $t + 1$ (Lee, 2012; Gelman et al., 2013). So after assimilating one observation at t, the posterior pdf could be propagated through the crop growth model to provide a prediction of the pdf of $\vec{x}$ at $t + 1$. This remark presents obvious advantages for applications where the state needs to be updated as new observations become available, and is fundamental for the development of methods such as the Kalman filter and its variants.

3.2. Variational approaches

Variational approach solves the analysis problem through the optimisation of a given criterion (minimisation of a cost-function). Fig. 2 depicts a basic flow chart of variational approaches. In variational approaches, some assumptions made. The first one is that all the statistics are assumed to be normal, and we arrive at the situation shown in Eq. (4). Under the assumption of weak non-linearities, the posterior is assumed normal, with a mean given by the value of $\vec{x}$ that minimises Eq. (4), and with a covariance matrix given by the inverse of the Hessian at the posterior mean point. The minimisation of $J(\vec{x})$ can be complicated if the state vector is large, and the use of gradient descent algorithms is preferred to global algorithms. In order to efficiently use gradient descent, the Jacobian of $J(\vec{x})$ is required, and it is given by

$$J'(\vec{x}) = \frac{\partial \mathcal{H}(\mathcal{M}(\vec{x}))^{\top}}{\partial \vec{x}}\mathbf{C}_{\text{obs}}^{-1}[\mathcal{H}(\mathcal{M}(\vec{x})) - \vec{y}] + \mathbf{C}_{\text{prior}}^{-1}[\vec{x} - \vec{\mu}]. \tag{5}$$

Differentiating further, we can calculate the Hessian as

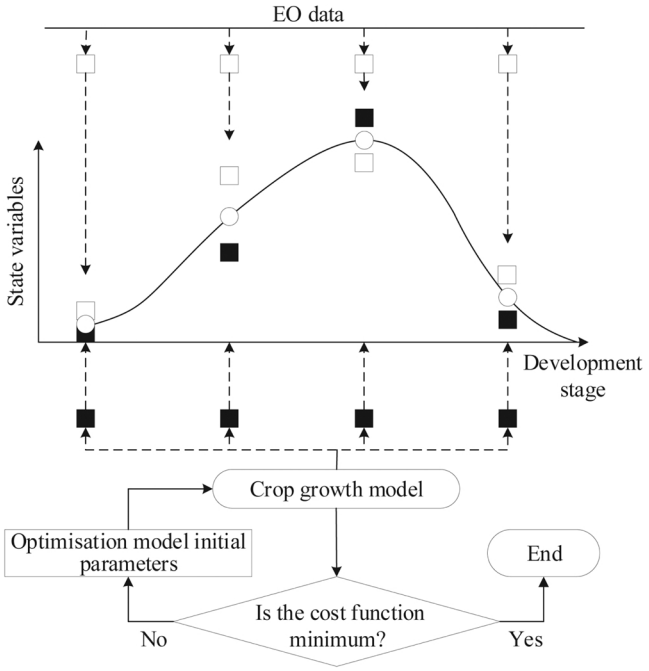

Fig. 2. Flow chart of variational methods.

$$J'(\vec{x}) = \frac{\partial \mathcal{H}(\mathcal{M}(\vec{x}))}{\partial \vec{x}} \mathbf{C}_{\text{obs}}^{-1} \frac{\partial \mathcal{H}(\mathcal{M}(\vec{x}))^{\mathrm{T}}}{\partial \vec{x}} + \frac{\partial^2 \mathcal{H}(\mathcal{M}(\vec{x}))}{\partial \vec{x}^2} \mathbf{C}_{\text{obs}}^{-1} [\mathcal{H}(\mathcal{M}(\vec{x})) - \vec{y}] + \mathbf{C}_{\text{prior}}^{-1}. \quad (6)$$

If the predictions of the model are a good representation of the observations (i.e. the value of $\mathcal{H}(\mathcal{M}(\vec{x})) - \vec{y}$ is close to zero), then the second term in the Hessian (which accounts for effect of non-linearities in the posterior uncertainty) can be ignored.

Approaches that assimilate observations without taking into account temporal dependency (e.g. Eqs. (4) and (7)) are usually termed 3DVar (Lorenc, 1986; Sasaki, 1970), whereas an approach that integrates the solution over time is called 4DVar (Le Dimet and Talagrand, 1986; Talagrand and Courtier, 1987).

We have so far assumed that all the uncertainty in the system comes from the imperfect observations. However, in addition to lack of definition of model parameters in the prior ($\mathbf{C}_{prior}$), errors in the model-drivers and structure, pragmatic model simplifications also influence the uncertainty of model simulation. We can model this model uncertainty as an additive normal term with zero mean and covariance given by $\mathbf{C}_{model}$. We can extend the formulation from Eq. (4) to account for this model error in the form of an extra term, a *weak constraint* (Sasaki, 1970; Zupanski, 1997):

Table 1
Representative research on variational approaches.

Cost function	Algorithm	CGM	Variables	EO data	References
4DVar	SCE-UA	WOFOST	LAI	MODIS, Landsat TM	Huang et al. (2015b)
	Powell	SWAP	LAI	MODIS	He et al. (2015)
	Powell	DSSAT + MCRM	NDVI, LAI, EVI	MODIS	Fang et al. (2011)
	AA	DSSAT	LAI	MODIS	Jin et al. (2016)
	AA	DSSAT + PROSAIL	NDVI	Landsat TM	Dong et al. (2013)
	SCE-UA	WOFOST + PPROSAIL	ρ	Landsat TM, Landsat OLI	Huang et al. (2019)
Root mean square error	SA	SUCROS + SAIL	ρ	Virtual reflectance	Guerif and Duke (2000)
	SCE-UA	SAFY	LAI	Landsat-8, MODIS	Dong et al. (2016)
	PSO	WOFOST	LAI	Landsat-8	Jin et al. (2015)
	PSO	WOFOST + PROSAIL	FAPAR	GF-1	Zhou et al. (2017)
Weighted sum of squared differences	SA	STICS	LAI	Landsat TM, SPOT, UAV	Jégo et al. (2012)
	MLS	DSSAT	LAI	ENVISAT ASAR, MERIS	Dente et al. (2008)
Least squares	SA	SUCROS + SAIL	TSAVI	SPOT, UAV	Launay and Guerif (2005)
	SA	SUCROS + SAIL	ρ	Measurements	Guérif and Duke (1998)
	SCE-UA	WOFOST	LAI	MODIS	Ma et al. (2013a)
	SCE-UA	ORYZA2000 + CLOUD	λ	ENVISAT ASAR	Shen et al. (2009)
	SCE-UA	SWAP	LAI	MODIS	Xu et al. (2011)
	PSO	WheatGrow + PROSAIL	VI	HJ-1A/B	Guo et al. (2018)
	ULM	WOFOST	LAI	SPOT, ERS, Radarsat	Curnel et al. (2011)
Vector angle	SCE-UA	SWAP	LAI, ET	MODIS	Huang et al. (2015a)
Mean absolute error	PSO	RiceGrow	LAI, LNA	ASD	Zhu et al. (2010)
	Powell	DSSAT	LAI	MODIS	Fang et al. (2008)
	Powell, SCE-UA	WOFOST	LAI	MODIS	Tian et al. (2013)
Relative error	PSO	WOFOST	LAI	HJ-1A/B	Liu et al. (2015)
	PSO	AquaCrop	CC, AGB	HJ-1A/B, RADARSAT-2	Jin et al. (2017)
	PSO	AquaCrop	CC	HJ-1A/B, Landsat-8	Silvestro et al. (2017)
	PSO	DSSAT	LAI, CNA	ASD	Li et al. (2015)
Penalty method	GA	SWAP	ET	Landsat ETM +	Ines et al. (2006)

Note: SCE-UA, PSO, MLS, Powell, SA, AA, GA, ULM, TSAVI, NDVI, EVI, ρ, λ, LNA, CC and CNA respectively represent shuffled complex evolution method developed at the University of Arizona, particle swarm optimisation, maximum likelihood solution, Powell's conjugate direction method, simplex algorithm, annealing algorithm, genetic algorithm, unconstrained Levenberg–Marquardt algorithm, transformed soil adjusted vegetation index, normalised vegetation index, enhanced vegetation index, band reflectance, backscatter coefficient, leaf nitrogen accumulation, canopy cover and canopy nitrogen accumulation. The same below.

$$J_{\text{obs}}(\vec{x}) + J_{\text{prior}}(\vec{x}) + J_{\text{model}}(\vec{x}) = \frac{1}{2}[\mathcal{H}(\mathcal{M}(\vec{x})) - \vec{y}]^{\top}\mathbf{C}_{\text{obs}}^{-1}[\mathcal{H}(\mathcal{M}(\vec{x})) - \vec{y}] + \frac{1}{2}[\vec{x} - \vec{\mu}]^{\top}\mathbf{C}_{\text{prior}}^{-1}[\vec{x} - \vec{\mu}] + \frac{1}{2}[\mathcal{M}(\vec{x}) - \vec{x}]^{\top}\mathbf{C}_{\text{model}}^{-1}[\mathcal{M}(\vec{x}) - \vec{x}]. \quad (7)$$

In Eq. (7) we still have a combination of Gaussians. By assuming that the posterior is also Gaussian as before, the mean will be a weighted combination of the fit to the observations, the fit to the prior pdf and the fit to the model, each of them balanced by their respective uncertainties. While the observational and prior uncertainties might be estimated reasonably well, the model error is usually not well defined and tends to require tuning.

In general, functionals like those presented in Eq. (4) or (7) are hard to minimise depending on the nature of the observation operators and models. For one, availability of tangent linear models and adjoint models is a non-trivial requirement (Giering and Kaminski, 1998). Additionally, for general non-linear observation operators or models, the function is not convex and may have multiple minima, which are problematic with local minimisation approaches based on gradient descent. Furthermore, if the prior covariance is ill-conditioned (large difference between the smallest and highest eigenvalues), the minimisation process will be slow, requiring many iterations to reach convergence. A solution to this is to use a pre-conditioner, or to solve a series of linear approximations to the problem. In that case, the approximate problem has a unique solution, and these approximations can be iterated (incremental 4DVar formulation, Courtier et al., 1994).

It is worth noting that in the crop growth DA literature, a wide range of function optimisers are used to solve a generic cost function problem (see Table 1). In some cases, global optimisers such as Genetic Algorithms (GAs) are used, but these optimisers are not efficient for problems characterised by many dimensions (e.g. many parameters), which we often find in regional applications. Gradient descent methods, on the other hand, are efficient and scalable local minimisers (so can get stuck in local minima), and require access to the gradient (Jacobian) of the model, which may not be available. In some cases, the gradient can be approximated by finite differences, but this approach will not scale to higher dimensions.

A summary of variational applications in the literature is shown in Table 1. It is immediately clear that a broad range of cost functions are used. The framework presented above deduces the cost function from Bayes' rule, where in the previous discussion all statistics were assumed normal. Using different cost functions results in different weightings of the evidence-model mismatch, which encode very different description of the statistics in observations and/or model. For example, a heavy tailed pdf for the observations (e.g. a Laplace or Student's *t* distribution) will tend to reduce the effect of outliers with respect to a Gaussian approximation, but the posterior will be far from Gaussian. Similarly, the vector angle method results in a complex likelihood that may be poorly approximated by a Gaussian. It would appear that in the literature these choices are done in an *ad hoc* manner, fundamentally to dampen or enhance the contribution of some observations to particular situations (the case of reducing the influence of outliers, or as a way of dealing with strong but unknown correlation structures in the observations). This results in difficulties in explaining the generality of the results to other data streams. Improvements in the characterisation and quantification of uncertainty would lead to more careful approximations of uncertainty in different DA frameworks.

In terms of linkages between observations and models, a predominance of LAI or FAPAR is in evidence. This is probably a consequence of LAI and/or FAPAR products being both widely available and having a clear representation or linking point within the crop growth model. Different authors opt for using off-the-shelf products, exploiting empirical relationships between e.g. vegetation indices (VIs) and either LAI or FAPAR, or using physical models to convert e.g. LAI to reflectance. In either of these approaches, it is important to understand the limitations of the observation operators, assimilating FAPAR is not necessarily the same as assimilating a VI, as in the former an interpretation of the reflectance has been made with a set of assumptions. It is important to note that the assumptions in the retrieval observation operator should be consistent with the assumptions within the cropthe coherence between reflectance and FAPAR is given only by the observation operator (RT model). Additionally, the use of SAR data appears less frequent, and although LAI is also widely derived from SAR data, other observables are presented (AGB). Some references have also used ET estimates.

3.3. Kalman filters

The Kalman filter assumes the prior distribution of state vector at time $t+1$ $\vec{x}_{t+1}$ is a Gaussian distribution with mean $\mathcal{M}(\vec{x}_t)$ and covariance matrix P_f :

$$p(\vec{x}_{t+1}) \propto \exp\left(-\frac{1}{2}(\vec{x}_{t+1} - \mathcal{M}(\vec{x}_t))^{\top}P_f^{-1}(\vec{x}_{t+1} - \mathcal{M}(\vec{x}_t))\right). \quad (8)$$

The observation $\vec{y}_{t+1}$ is assumed to have a Gaussian pdf with mean $\mathcal{H}(\vec{x}_{t+1})$ and covariance matrix R:

$$p(\vec{y}_{t+1}|\vec{x}_{t+1}) \propto \exp\left(-\frac{1}{2}(\vec{y}_{t+1} - \mathcal{H}(\vec{x}_{t+1})^{\top}R^{-1}(\vec{y}_{t+1} - \mathcal{H}(\vec{x}_{t+1}))\right). \quad (9)$$

If the linear dynamical system (both $\mathcal{H}$ and $\mathcal{M}$ are linear) is further modelled as a Markov chain that the state vector is conditionally independent of all earlier states given the immediately previous state,

$$p(\vec{x}_t|\vec{x}_0, ..., \vec{x}_{t-1}) = p(\vec{x}_t|\vec{x}_{t-1}), \quad (10)$$

then after a series of derivations (refer to Anderson and Moore, 2012 for details), it can be shown that the posterior pdf $p(\vec{x}_{t+1}|\vec{y}_{t+1})$ of state vector $\vec{x}_{t+1}$ is also Gaussian with mean and covariance matrix as

$$E(\vec{x}_{t+1}^{a}) = \mathcal{M}(\vec{x}_t) + K(\vec{y}_{t+1} - \mathcal{H}(\mathcal{M}(\vec{x}_t))), \quad (11)$$

$$\text{Cov}(\vec{x}_{t+1}^{a}) = (I - K\mathcal{H})P_f, \quad (12)$$

where the superscript a stands for *a posteriori*, and K is

$$K = P_f\mathcal{H}^{\top}(\mathcal{H}P_f\mathcal{H}^{\top} + R)^{-1}. \quad (13)$$

If the state vector $\vec{x}_t$ represents the state of the system at some time t, from an initial prior estimate of this state (assumed Gaussian), and a given observation operator $\mathcal{H}$ between the state and the observations $\vec{y}_t$ at the current time, we can solve Eq. (4) which ignores the model error (e.g., drivers and model structures) of crop growth model to obtain the *a posteriori* pdf of the state $\vec{x}_t$ at t. This pdf can then be propagated by the crop growth model $\mathcal{M}$ to time $t+1$ to provide an *a priori* state vector pdf estimate at this new time step. To account for model error, some additional uncertainty can be added to the propagated state (in the same way as the weak constraint in the 4DVar approach introduced earlier). This procedure is repeated sequentially for each new time step. The Kalman filter (Jazwinski, 2007) provides a recursive expression for the sequential update of the state vector: new observations are assimilated using the propagated state (and associated uncertainties) from a previous time step as a prior.

The Kalman filter equations only hold with linear crop growth models and linear observation operators and assume all statistics are Gaussian. However, dynamic crop models are often not linear, as the growth process is affected by many factors, including light, temperature, water and fertiliser. This process cannot be adequately simulated by linear models. As a result, a standard Kalman filter cannot be used directly. If either the observation operator or the crop growth model is

non-linear, then a linear approximation of the model can be performed by using Taylor series expansion, which leads to the Extended Kalman filter (EKF) (Jazwinski, 2007).

The lack of access to the gradient of $\mathcal{M}$ or the computational complexities in calculating the propagation equations for large dimensional problems can be solved by propagating an ensemble of state realisations through the crop growth model, and from these, calculating the prior covariance matrix for the next step. This approach is the Ensemble Kalman filter (EnKF, Evensen, 2003), which is essentially a Monte Carlo approximation of the Kalman filter and makes the assumption that all probability distributions involved are Gaussian. EnKF use an ensemble that is a sample from the prior distribution to calculate the covariance of the prior state vector,

$$X = [\vec{x_1}, ..., \vec{x_N}], \tag{14}$$

an $n \times N$ matrix whose columns are the ensemble members. From Eq. (14), the ensemble covariance P_e can be obtained. There are two common methods to generate the ensemble of initial state of the crop growth model, one based on state variables and the other based on initial conditions and parameters (Huang et al., 2016). The observation ensemble is Y,

$$Y = [\vec{y_1}, ..., \vec{y_N}], \tag{15}$$

an $m \times N$ matrix. Taking the example of crop model assimilation with earth observations, each column $\vec{y_i}$ consists of the earth observation $\vec{y}$ plus a random vector from the m-dimensional normal distribution $N(0, R)$. From Eq. (15), the ensemble covariance of observations R_e can be obtained. The analysed matrices of ensemble states (mean value of the posterior pdf) is given by

$$X_{t+1}^a = \mathcal{M}(X_t) + P_e\mathcal{H}^T(\mathcal{H}P_e\mathcal{H}^T + R_e)^{-1}(Y_{t+1} - \mathcal{H}(\mathcal{M}(X_t))). \tag{16}$$

If the earth observation data is the state variable of the model, then the observation operator $\mathcal{H}$ is an identity matrix, and Eq. (16) can be simplified as

$$X_{t+1}^a = \mathcal{M}(X_t) + p_e(p_e + R_e)^{-1}(Y_{t+1} - \mathcal{M}(X_t)) \tag{17}.$$

Several implementations are available as shown in Table 2. The standard EnKF method tends to reject observations in favour of the ensemble forecast in the late period of data assimilation, which could lead the analysis to deviate incrementally from the reality, which is referred to as *filter divergence* (Schlee et al., 1967; Fitzgerald, 1971; Burgers et al., 1998; Ines et al., 2013). To reduce the effect of filter divergence, an inflation factor is often adopted to enlarge Kalman gain (Lin et al., 2008; Huang et al., 2016).

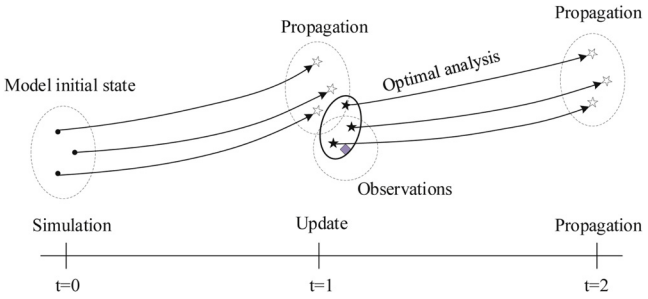

Fig. 3. Flow chart of Kalman filtering methods.

Satellite-derived products can provide direct, uncertainty-quantified estimates of components of the state vector (e.g. LAI) that can be immediately linked to model predictions. If the statistics of the error of the data product are Gaussian, Kalman filters are a good choice. Since most crop growth models are non-linear, the use of EnKF is a practical way to assimilate products. However, it is worth noting that most crop growth models can be well approximated by a local linear model around when updating the state. If direct satellite measurements (e.g. reflectance, radiance or backscatter) are assimilated, then the RT models might also be very non linear, but local linear approximations may be feasible. If these approximations are available, by e.g. using emulators (Gómez-Dans et al., 2016), then using the Extended Kalman Filter (EKF) might be an efficient alternative to the the EnKF.

Unlike variational approaches (e.g. 4DVar which optimises model parameters), Kalman filtering is a sequential method to estimate the state vector at different time points. Fig. 3 depicts a basic flow chart of Kalman filtering methods. It uses a series of measurements observed over time containing statistical noise and other inaccuracies, and, by sequentially estimating a joint probability distribution over the variables for each time frame, it produces estimates of unknown variables that tend to be more accurate than those based on a single measurement alone. An important distinction from variational approaches is that filtering approaches are causal: they only use information from the past to assimilate an observation at the current time. In variational systems, information from the whole assimilation temporal window needs to be used, resulting in a more constrained problem compared to filters. Filters, on the other hand, allow on-line updating and near real time operation. The common point between 4DVar and Kalman filter is that they are both based on Gaussian assumption and Bayes' rule. Once the

Table 2
Representative research on filtering approaches.

Algorithm	CGM	Variables	EO data	References
CGKF	SWAP	LAI, ET	MODIS	Vazifedoust et al. (2009)
	MCWLA-Wheat	LAI	GLASS LAI (MODIS-based)	Chen et al. (2018)
EnKF	WOFOST	LAI	MODIS	Wu et al. (2011), Zhao et al. (2013), Zhu et al. (2013)
	WOFOST	LAI	Landsat ETM+	Li et al. (2014)
	WOFOST	LAI	MODIS, Landsat TM	Huang et al. (2016)
	WOFOST	LAI	HJ-1A/B	Ma et al. (2013b), Cheng et al. (2018)
	WOFOST	LAI	PROBA/CHRIS	Wang et al. (2013)
	WOFOST	LAI	SPOT, ERS, Radarsat	Curnel et al. (2011)
	WOFOST	SM	ERS, EUMETSAT	de Wit and van Diepen (2007a)
	WOFOST	SM	SMOS	Chakrabarti et al. (2014)
	WOFOST	LAI, SM	Synthetic data	Pauwels et al. (2007)
	WOFOST	LAI, SM	AMSR-E, MODIS	Ines et al. (2013)
	DSSAT	LAI, SM	MODIS, SMOS	Nearing et al. (2012)
	DSSAT	LAI, VTCI	Landsat TM, ETM+ and OLI	Xie et al. (2017)
	SAFY	LAI	HJ-1A/B, Landsat-8	Silvestro et al. (2017)
EnSRF	WheatGrow	LAI, LNA	HJ-1A/B, Landsat TM	Huang et al. (2013)
	DSSAT	LAI, SM	MODIS, AMSR-E	Mishra et al. (2015)
	SWAP	SM	SMOS	Singh and Panda (2015)

Note: CGKF, EnKF, EnSRF, VTCI represent constant gain Kalman filter, ensemble Kalman filter, ensemble square root filter, vegetation temperature condition index.

filter has been run for some time, the filter can then be run backwards to update the initial filter estimate, in what is called a smoother. Algorithms exist for the Kalman smoother (Briers et al., 2009), which can be shown to be equivalent to the 4DVar with a weak constraint approach introduced in Eq. (7) (Fisher et al., 2005).

3.4. Bayesian Monte-Carlo approaches

The previous two sections describe DA methods that either have a direct analytic solutions (e.g. the Kalman filter and derivatives), or can be solved by minimising a cost function. In either case, the use of Gaussian distributions results in a solution that can be encoded as a mean vector and a covariance matrix. However, with non-linear observation operators and crop growth models, or indeed where the uncertainties in the model or the observations are non-Gaussian, assuming normality in the posterior might be a poor choice. In these cases, approaches based on sampling are preferred.

In these sampling approaches, samples from the posterior pdf are drawn as the solution, allowing the solution to be e.g. non-normal and multimodal. The most general sampling approach is Markov chain Monte Carlo (MCMC) (Gilks et al., 1995), using a Markov chain to produce samples from the posterior pdf. The way MCMC works is by, firstly identifying a Markov chain (the first MC in MCMC) whose stationary distribution is the posterior of interest, then sampling from this Markov chain until it converges to an equilibrium distribution. As a result, MCMC is essentially sampling from the posterior distribution of interest. This is a very general approach that will work for any problem, provided that the chain is let to run for a sufficient number of iterations and that the chain converges to the required posterior pdf. Convergence of the chain is hard to diagnose, and a number of rules of thumb are usually deployed (Cowles and Carlin, 1996), e.g., the widely used R hat indicator (Gelman et al., 2013). MCMC methods are practical for one-off inferences and where the dimensionality of the problem is not very high. If the dimensionality is very high, MCMC methods are slow to explore the solution space, and convergence is hard to achieve in practical time scales.

The causal equivalents of MCMC are sequential Monte Carlo methods, such as particle filters (PF). Fig. 4 shows the basic steps of a Metropolis–Hastings MCMC and Particle filters algorithms. Particle filters allow the propagation of non-Gaussian distributions through complicated crop growth and/or observation models, and show some potential for RS-crop model DA compared with the widely used EnKF (Jiang et al., 2014; Machwitz et al., 2014; Chen and Cournède, 2014). A number of implementations of these filters are straightforward extensions of the basic MCMC algorithms (Dowd, 2006, 2007), while others are more directly based on importance sampling (van Leeuwen, 2009; Ristic et al., 2004; Arulampalam et al., 2002). An important consideration for particle filters is that in order to reliably describe the posterior pdf, a large number of particles may be required. This is an even more pressing need when the dimensionality of the problem increases. Addressing this problem in particle filters is an active area of research (Ades and Van Leeuwen, 2015; Ades and van Leeuwen, 2013; van Leeuwen, 2010).

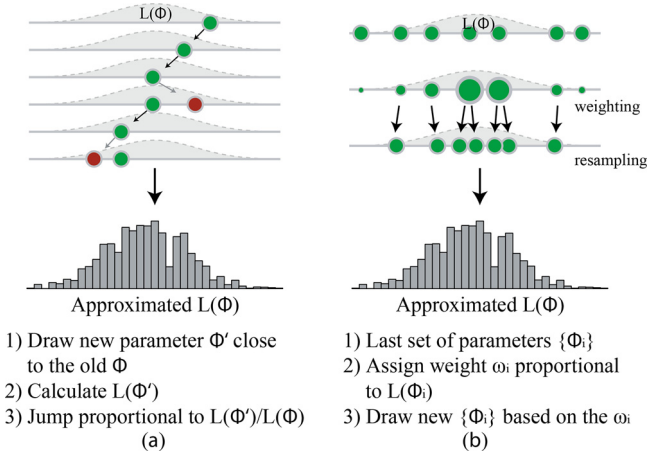

Fig. 4. Illustration of Metropolis–Hastings MCMC and Particle filters algorithms. The light grey shapes depict the target distribution (posterior). Circles depict parameter combinations within the algorithm. (a) A Metropolis-Hastings MCMC sampler proposes a new value conditional on the last, and accepts (green) or rejects (red) according to the ratio of the point-wise likelihood approximations. (b) Sequential Monte Carlo samplers start with an ensemble of parameter values, weight them according to their approximated point-wise likelihood values, and potentially draw new values from the last ensemble according to those weights (Hartig et al., 2011).

In practice, the MCMC methods or particle filters have been widely applied to studies on hydrologic and land surface models (Evensen, 1994; Vrugt et al., 2003, 2008; Moradkhani et al., 2005, 2012; Yang et al., 2008; Matgen et al., 2010; Montzka et al., 2011). The approach appears to be promising for non-linear crop growth models, as shown in Table 3, and some applications have shown encouraging results. The MCMC methods seem to be effective and efficient for crop model parameter estimation and uncertainty analysis (Makowski et al., 2002; Dumont et al., 2014; Iizumi et al., 2009), examples where timeliness and data volumes are not large. Ultimately, the full power of sampling methods stems from their ability to cope with non-Gaussian, non-linear generic problems, and in this respect, the bigger hurdle might lay with the requirements to parameterise e.g. the prior pdf or the likelihood function, rather than with the method of choice.

3.5. Choice of DA methods

The previous sections open a landscape of DA methods, and immediately the question arises of which is the most adequate method to use for a particular application. Fig. 5 depicts a simplified decision tree for DA methods choice strategy.

A first decision would be based on timeliness: if near real-time inferences, or even forecasts of harvest time yield during the growing season, are required, then filters are the obvious choice, although variational or sampling methods might be used within an assimilation window. These first inferences might be refined after harvesting (similar to reanalysis in meteorology, Parker, 2016), either by updating the filtered estimates to produce a smoothed inference, or equivalently by running a variational inversion (Fisher et al., 2005). Clearly, this could be a suitable strategy for inferences from past campaigns. EnKF predicts yield through optimising the state variables (e.g. LAI or SM) during the growing period of the crop, not only near past. Because EnKF is based on a Markov chain, all past observations will be used implicitly, with recent observations being more closely weighted. 4DVar fits the model to all the observations within the assimilation window, and uses the propagates the solution through the crop model to forecast yield. The general set-up of the EnKF makes its extension to within-season forecasting straightforward, whereas variational methods need to consider the size of the assimilation window and how that would affect predictions.

Secondly, an additional decision might be made on the basis of statistical, model or observation operator characteristics. The standard Kalman filter can be used if the observations are direct measurements of the state (e.g. LAI, SM, AGB) or linear transformations of the state, and the crop model can be assumed to be linear too. Usually, the crop growth model is assumed to be highly non-linear, which calls for approaches like EnKF (de Wit and van Diepen, 2007a; Ines et al., 2013) or particle filters (Machwitz et al., 2014). A more pragmatic take would consider whether the crop growth model can be assumed locally linear when it updates the state between adjacent time steps, in which case the standard Kalman filter might be a good choice, particularly if efficient emulators of the crop growth that provide access to the Jacobian

Table 3
Representative research on sampling approaches.

Algorithm	CGM	Variables	EO data	References
DREAM	STICS	AGB	Measurements	Dumont et al. (2014)
M-H	PRYSBI	heading day, yield	Statistics	Iizumi et al. (2009)
PF	DSSAT	LAI	HJ-1A/B	Jiang et al. (2014)
	APSIM + PROSAIL	ρ	RapidEye	Machwitz et al. (2014)
CPF	LNAS, STICS	LAI, AGB, etc.	Measurements	Chen and Cournède (2014)

Note: DREAM, M-H, PF, CPF, PRYSBI represent differential evolution adaptive Metropolis, Metropolis–Hastings, particle filter, convolution particle filtering, Process-based Regional-scale rice Yield Simulator with Bayesian Inference.

are available.

Although reflectance cannot be simulated by crop models directly, one can couple the crop model predictions of e.g. LAI or soil moisture with physical model to simulate the observed satellite measurements (e.g. reflectance, backscatter, ...). As with the comments in the last paragraph, local linearisations of the non-linear physical models may be used to benefit from the simpler linear Gaussian DA approaches. In some cases, very simple parameter transformations are able to quasi-linearise an observation operator, which means that the problem is solved in transformed space and the solution is then presented in real units space with the posterior pdf not being Gaussian in this case (Weiss et al., 2001; Lewis et al., 2012).

The use of variational schemes is hampered by the need to have access to the gradient of the crop growth model and/or the observation operator, which is not always practical. Pragmatic approaches to overcome these limitations are the use of look-up tables (LUTs) for the models, often used in biophysical parameter retrieval from EO observations, e.g. Weiss et al. (2000), which can also be used with the crop growth model. Hank et al. (2015) use an ensemble of model trajectories, which amounts to a LUT for model trajectories. The ensemble members that are most consistent with the observations are selected in this way. Approaches based on look-up tables are easy to implement and scale to situations where the crop growth models and/or the observation operators need to be evaluated many times.

If the statistics are non-normal and the crop growth model and the observation operator are non-linear, then sampling methods are the recommended option. However, the computational cost of these methods make them unsuitable for high dimensional applications, and even then, a large computational effort might still be required. Nevertheless, even in cases where sampling methods may be impractical, they provide a benchmark to test the assumptions made to use some of other methods. It is also important not to forget that in many cases, non-linearities in models are not too large, and particle methods might not be needed. Ziehn et al. (2012) show that for a complex terrestrial ecosystem model, both a variational and an MCMC approach converge to the same global minimum, and provide nearly identical representations of the posterior pdf, but with the variational approach being several orders of magnitude faster than MCMC. Using 4DVar to assimilate and then using MCMC to verify the assimilation at limited point is a promising solution for large area assimilation.

Finally, a further comment is that, throughout the previous discussion, we have always assumed that there is no bias between the model and the observations. If this is not the case and the model predictions are very far from the observations, the Bayesian paradigm will in effect weight the observations and the predictions, and produce an analysis that is a weighted average of both terms. This disparity can be due to the predictions from a poorly calibrated model that fails to provide a good representation of the crop development, or can arise when the observations have biases due to different assumptions in the retrieval scheme (such as spatial scales, see the next Section), or due to unfiltered defective retrievals (outliers) in the data. If these conditions arise, and the bias is not removed, the analysis (combination of observations and model predictions) might be an unrealistic weighted average.

4. Challenges in data assimilation applied to crop monitoring

4.1. Pre-DA considerations

4.1.1. Choice of simulation spatial and temporal scale

One of the most challenging aspects of the use of RS-crop model DA stems from the spatial heterogeneity of croplands with respect to typical remote sensing spatial resolutions. The choice of simulation scale can vary by several orders of magnitude depending on the application. For some regional applications (e.g. national region), a coarse grid can be sufficient, whereas for local/field scale a finer grid might be required (around ~km for provincial scale, 10s to 100s m for county scale, m to 10s m for plot scale). It is important to consider that the limitations of

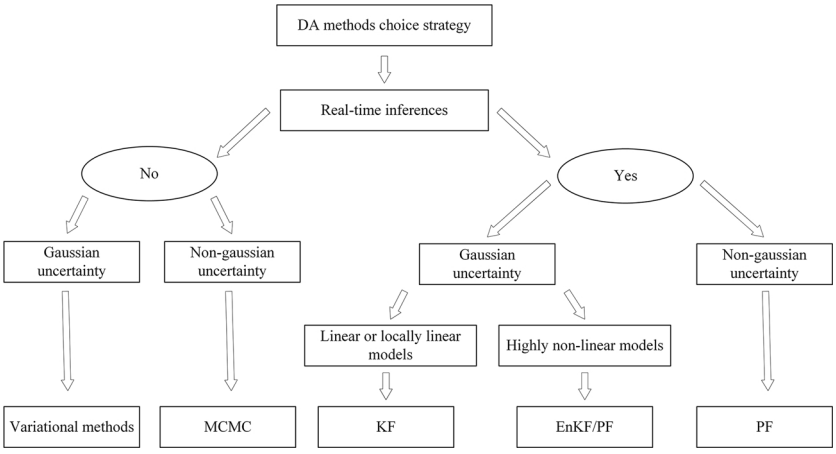

Fig. 5. Decision tree for DA methods choice.

the model might make it more or less suitable for some spatial scales as the model may lack important processes that have a strong local impact for example horizontal water transport at high spatial resolution. Crop models can be adapted to the relevant spatial scale. For example, a crop model may not be able to reproduce some between- or within-field patterns, or the model parameterisation may require much more caution to account for different crop varieties, different management practices (e.g. irrigation, fertilisation) and so on. In the DA context, we can picture the role of DA as correcting the model predictions: the observations help guide the imperfect model towards the actual development of the crop. In this sense, the model and the state both depend on the application. The increase of spatial resolution results in a requirement for crop growth model parameters and other input variables (e.g. meteorological inputs or soil maps) at a similar spatial resolution in order to capture the inherent variability of the system. Perhaps a useful illustration of this situation would consider that at moderate to large scale (m to km scale), any model will be poorly parameterised, and input meteorological data will usually poorly represent local weather conditions. The role of DA in this case would be to make the model use observations as symptoms of crop evolution, which are at much finer scale than the model drivers and parameters, tracking variations in the crop development that compensate for the limitations in the model drivers, parameters and model itself.

Another important consideration is on the temporal aspect. Although different processes have different temporal scales, crop growth models tend to operate on daily scales. Access to these daily measurements is thus a pre-requisite for running the model. In an operational scenario, a DA system would track the crop development up to a given time, in which case the state of the crop would be defined. Then, the crop growth model could be run until harvesting using e.g., an ensemble of historical meteorological data (Lawless and Semenov, 2005; Hansen et al., 2006). In these cases, the inherent uncertainty in the state after the last assimilation window is propagated through a model which is driven by uncertain meteorological drivers (Fig. 6). In recent years, major advances have occurred in the area of seasonal weather forecasting (Meza et al., 2008; Wheeler et al., 2007; Doblas-Reyes et al., 2013; Swinbank et al., 2016). Seasonal forecasts can be used to derive an ensemble of plausible weather states at the General Circulation Models (GCMs) temporal and spatial resolution. For example, ECWMF can forecast up to 15 days in advance with a spatial resolution of 25 km, depending on which daily meteorological element can be produced. If medium and long-term forecast data are used, we can predict crop yield in advance 1–3 months before harvest. However, these inferences, often stored in the form of ensembles need to be downscaled to the usual daily inputs required by CGMs (temperature, precipitation, etc.). This can sometimes be done by using so-called weather generators, which tend to produce an ensemble of possible meteorological driver trajectories (Semenov and Doblas-Reyes, 2007; Marletto et al., 2007; Apipattanavis et al., 2010; Lv et al., 2013). In addition to statistical downscaling methods such as weather generators, the dynamic downscaling method based on regional climate models (RCMs) and the combination of these two are among the future study direction of the field. Important programs in the field include ENSEMBLES and CORDEX (Van der Linden et al., 2009; Giorgi et al., 2009).

4.1.2. Crop model calibration

Before carrying out any DA procedure, a CGM should be carefully calibrated with observable biophysical parameters including LAI, yield and/or biomass distribution in different organs (e.g. Ceglar et al., 2011). Typically, these calibrations are done with ground observation instead of remote sensing observations, mainly due to the scaling difficulty in remote sensing products and their associated uncertainties (see next two subsections for more details). One may argue for the spatial limitation of ground observations, however typical values of CGM parameters fall within very limited range of values (Boogaard et al., 2014) and we expect the parameter values not to vary dramatically away from the calibrated values. This is, indeed, where DA can demonstrate its capability as a promising solution to take into account such scale-dependent bias as discussed in the previous subsection.

4.2. Uncertainty characterisation

The uncertainty of the assimilation system includes the uncertainties in model errors (e.g., drivers and model structure), model parameters and observations.

4.2.1. Uncertainties in model errors

All of these uncertainties are difficult to be quantitative estimated, especially model structure. On the one hand, the model missed some model structure and process which should be considered, for not fully understanding the physical process. On the other hand, model is a simplification and abstraction of physical processes so it can't accurately simulate the real world. Uncertainties in driver (e.g. temperature, radiation, rainfall, vapor pressure, wind speed) often arise from

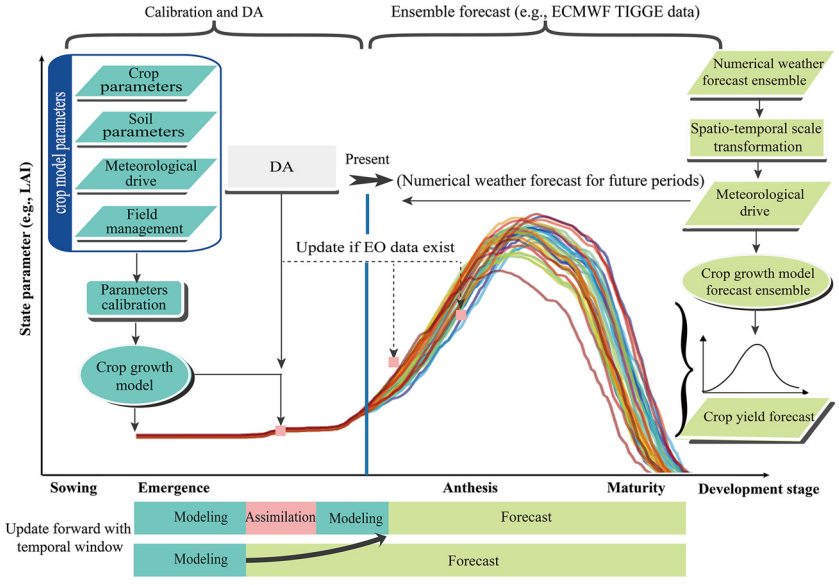

Fig. 6. DA with numerical weather forecast.

interpolation of point measurements to cover large areas. Interpolation approaches that provide a local estimator of uncertainty are available, usually (but not always) based on Kriging (Wilson and Silander, 2014; Ließ et al., 2012; Poggio and Gimona, 2014). These approaches are usually computationally costly, and are thus not routinely available. Local experiments using high accuracy measurements (e.g. independent meteorological stations) can be used to assess uncertainty in the interpolated data. Whether model errors are important depends on the research objective. For example, the model error (e.g., the drivers: rainfall) usually has been taken into account in the soil water balance of WOFOST model (de Wit and van Diepen, 2007b). However, errors in model parameters such as TDWI and SPAN have been taken into account in the data assimilation process (Huang et al., 2015b, 2016).

4.2.2. Uncertainties in model parameters

Probabilistic calibration of the crop growth model with detailed, multi-variate *in situ* data and a reliable Bayesian framework can provide an indication of the different sources of uncertainty. In reality, this is just an application of the methods introduced in Section 3, but now the object of interest is not the state of the system but for example the model parameters, or even the magnitude of the sources of uncertainty. Specifying a prior pdf for model parameters, as well as prior information of driver uncertainty, the model can be made to fit the *in situ* observations updating the prior pdf on parameters and driver uncertainties. Standard approaches to this problem rely on the use of MCMC methods (Ceglar et al., 2011; Van Oijen et al., 2011, 2005; Patenaude et al., 2008; Lehuger et al., 2009; Makowski et al., 2002; Dumont et al., 2014; Iizumi et al., 2009). While these approaches are computationally costly, they are often only required once, and provide a much more flexible way of encoding prior information with arbitrary pdfs. It is important to gather as much ground data as possible so as to constrain the largest possible region of parameter space. This should be checked after the calibration by assessing the reduction of uncertainty in parameters due to the observations used for calibration. Compensatory effects in parameters (where parameters or processes compensate for each other with respect to observations) should be identified after the calibration, as these effects can be used to simplify the DA problem (by prior specification), or may lead to model improvements. The posterior parameter pdf provides a lower bound in the model uncertainty $\mathbf{C}_{CGM}$ introduced in Section 3, which can be used to produce ensembles of model predictions that incorporate the calibration uncertainty. Related to this point, an analysis of the statistical properties of the posterior pdf can lead practitioners to decide that simplifications (e.g. assume that the parameter pdf is Gaussian) are acceptable, or at any rate, the analysis might provide some information on the price paid for common simplifications. Parameters error estimated from the posterior probability distribution by MCMC can be used to quantitatively determine the $\mathbf{C}_{prior}$.

4.2.3. Uncertainties in observations

The uncertainties in the observations are also of great importance, and general guidelines for uncertainty production and reporting are being established by the community (Povey and Grainger, 2015; Merchant et al., 2017; Kaminski et al., 2017). There are however many EO-derived products with poor or no uncertainty information available, and it is up to the researchers to provide an indication of uncertainty. This could be achieved by comparing a limited dataset of *in situ* measurements with the EO-derived estimates (Dente et al., 2008; Huang et al., 2015b), although it is hard to characterise the generality of this estimate. Ultimately, a reason for this lack of uncertainty stems from the fact that products are derived from intermediate products, so leaf area index is often derived from surface reflectance, and if the surface reflectance product does not provide an uncertainty estimate, this will need to be prescribed (Lewis et al., 2012; Laurent et al., 2014), although some efforts to derive it from the statistical properties of the image have been reported (Mousivand et al., 2015). It is thus important that all intermediate products have uncertainty estimates, or that a more direct coupling of the at-sensor measurements (e.g. top of atmosphere radiance) and the parameters of interest is used. The at-sensor measurements can be calibrated much more accurately than those of intermediate products, and the at-sensor uncertainties can then be propagated through the entire chain (Laurent et al., 2013; Lewis et al., 2012).

4.3. Scale mismatch between observations and models

The satellite derived biophysical parameters are generally not the same variables as the simulations from crop growth models. A cause of this discrepancy is satellite products are derived from heterogeneous pixels with a multitude of landcover types and/or vegetation states, and under the assumption that a single variable (e.g. LAI) is able to explain all this variation.Additionally, crop growth models are relatively successful in simulating the potential growth, as affected by climate and crop characteristic, and may provide an unrealistic prediction of the current state of the vegetation. Also the growth inhibiting effects of water shortage, oxygen shortage, salinity excess and nutrient shortage can be simulated quite well with current crop growth models. However, the growth reduction due to weeds, pests, diseases and temperature stresses are still difficult to simulate. Satellites measure the actual growth conditions, which includes the total effect of all growth reducing factors. This would cause a mismatch between the crop growth simulations and the crop growth measured by satellites (Hoefsloot et al., 2012).

The complexity of agricultural landscapes can result in the characteristics of different processes that are observed at various spatial or temporal scale, which can be easily adjusted. For example, daily air temperature measurements at a fine scale can be averaged spatially to provide an accurate estimate of temperature at a coarser spatial scale. Other processes or parameters might require more complex scalings: interpreting coarse spatial resolution surface reflectance observations using LAI results in the retrieved magnitude being usually lower than that obtained by estimating LAI from high resolution surface reflectance that are then spatially averaged and matched to the coarse resolution estimates. The bias is a consequence of the non-linear transformation of LAI to reflectance and the heterogeneity of the landscape (Liang, 2000; Garrigues et al., 2006).

Approaches to solving the scale problem follow two main strategies: the model adaptation school suggests a revision of processes in models to accommodate the relevant scales of the observations (Gao et al., 2001; Li et al., 1999; Raffy, 1992); and the scale transformation school advocates for approaches that minimise the scale-induced bias (Chen, 1999; Garrigues et al., 2006; Jiang et al., 2018; Martínez et al., 2009; Miller et al., 2004; Raffy, 1992; Wu et al., 2015, 2011). The latter process could be implemented either through upscaling (from high spatial resolution to coarse) or downscaling (disaggregating coarse spatial resolution data to high spatial resolution). The downscaling is a complicated process that requires approximations and extensive prior knowledge (Duveiller et al., 2011), and it might not be practical. Although, examples of downscaling practices through combination with infrequent high resolution data using double logistic or Kalman filter transformation can result in improved behaviours of the DA system on regional scales (Huang et al., 2015b, 2016, 2019). Another stream of studies lies between the two aforementioned schools is the use of bias-reduced spatial subset. Instead of using all available pixels in the study scene, these studies (de Wit et al., 2012; Duveiller et al., 2015) choose a spatial subset of more adequate time series in which the bias is already reduced. They provide a pragmatic solution to avoid modelling the scale-dependent bias and focus on areas where the analysis and the crop DA is more likely to succeed.

5. Future development and perspectives

5.1. Seamless DA for crop monitoring and yield forecasting

Limitations on the technology and, more fundamentally, in the processes that give rise to the observations captured by satellites result in an incomplete assessment of croplands. Combination of sensors might result in better monitoring capabilities of croplands. An obvious improvement is mitigating the vulnerability of optical data to cloud cover: having more sensors results in increased opportunity of observing land, even in cloudy regions (Claverie et al., 2018; Skakun et al., 2017; Huang et al., 2015b, 2016, 2019). The Sentinels programme from Copernicus includes SAR (Sentinel 1), optical high resolution (Sentinel 2) and coarse resolution optical and thermal (Sentinel 3/OLCI and Sentinel3/SLSTR) constellation of sensors. With the Landsat programme in the US, the combination of all these sensors provides frequent coverage of most of the Earth's landmass, with a richness of information that is revolutionary. DA offers the techniques to combine observations from different sensors in a consistent manner, providing a practical implementation of the virtual constellation concept (Wulder et al., 2015; Gómez-Dans et al., 2016).

Combining the observations from different sensors would also result in reduced uncertainty in retrieved crop parameters by virtue of combining more evidence. In this aspect, the DA system would assimilate all available observations, providing a much stronger system than using a single sensor or product. A condition to this success is the consistent pre-processing of all observations, which includes common assumptions and full uncertainty quantification. A particular difficulty here is to make the physical models consistent across spectral domains: while canopy modelling in the optical and thermal is mostly consistent due to the similar range of wavelengths, SAR physical modelling is quite different, requiring that some consistency checks are introduced in mixed processing chains.

Many DA studies have focused on the assimilation of LAI. One reason for this is that LAI can be an effective diagnostic of crop status, serving as an indicator of leaf abundance, as well as of phenological stage, and acting as a useful proxy to different management approaches, impact of pests and other stresses. However, having a single point of contact between the observations is limiting, as LAI can only provide an integrated effect of e.g. the effect of drought or pests. The assimilation of other variables, such as ETa/ETp or soil moisture can be used to complement LAI observations, providing an indication of crop stresses (Olioso et al., 1999, 2005; de Wit and van Diepen, 2007a; Ines et al., 2013). GLEAM (Global Land Evaporation Amsterdam Model) is a set of algorithms dedicated to the estimation of terrestrial evaporation and root-zone soil moisture based on satellite data (Miralles et al., 2011; Martens et al., 2017). In 2017, a third version of the model (GLEAM v3) has been developed, and two datasets that differ only in their forcing and temporal coverage was produced using this version of the model that are available. These two datasets can be used for crop DA study. SAR data can also provide a complementary observations in regions with high cloudiness (Dente et al., 2008), and backscatter has also been related to above ground biomass (Prévot et al., 2003; Inoue et al., 2002; Molijn et al., 2014; Shao et al., 2001; Toan et al., 2017; Nearing et al., 2012; Betbeder et al., 2016). VOD (vegetation optical depth) can measure attenuation of surface microwave emission due to the overlying vegetation is proportional to the density of the canopy and to its water content. Therefore, it has the potential to provide information about agro-ecosystems. The yield-VOD relationship has been explored by using principal components regressions (Chaparro et al., 2018). Solar-induced chlorophyll fluorescence (SIF) provides a direct link to instantaneous photosynthetic activity (Guanter et al., 2014; Guan et al., 2016; MacBean et al., 2018), and is now publicly available from a number of missions (Joiner et al., 2011; Guanter et al., 2012). SIF is emitted in the spectral range of 640-850 nm and is characterised by two peaks centered at around 685 nm and 740 nm, respectively (Zhao et al., 2018; Porcar-Castell et al., 2014). SIF can serve as a direct and non-invasive indicator of the functional status of photosynthetic machinery (Meroni et al., 2009). In a study to link spaceborne SIF retrievals from the Global Ozone Monitoring Experiment-2 satellite and United States crop yield by Guan et al. (2016), it was found that the SIF-based approach accounting for photosynthetic pathways (i.e. C3 and C4 crops) provides the best measure of crop productivity among various traditional crop monitoring approaches. More recently, Norton et al. (2018) demonstrated that remote sensing derived SIF could be used to optimise the process-based terrestrial biosphere model and the uncertainty in estimates of gross primary production (GPP) was largely reduced. There is no crop growth model can simulate chlorophyll fluorescence, thus SCOPE (Soil-Canopy spectral radiance Observations, Photosynthesis, fluorescence, temperature and Energy balance) model would be used in this study. For example, firstly, EO derived SIF is assimilated into SCOPE model to obtain assimilated GPP. Then, the assimilated GPP is assimilated into WOFOST model to simulate grain yield.

It is worth noting that the rich spectral sampling capabilities of Sentinel-2 can provide additional information on leaf pigments such as chlorophyll concentration that show promising links to photosynthetic activity (Gitelson et al., 2006; Croft et al., 2017; Delloye et al., 2018). In order to fully exploit these new parameters, more researches are needed in how they relate to processes already present in the crop growth models, and how to best interface the new observations to the models.

Extending the richness of the observation products results in additional constraints to the model space, as different processes are made to track different sets of observations. In this sense, consistency between different observations is crucial, as is accurate estimation of uncertainties associated with the various observational inputs.

5.2. Extending assimilation to large area and near real-time

More complex models, both for simulating crop growth and development as well as for observation operators, and the increased resolution of observations, both in time and in space, result in an increase computational cost for contemporary DA systems. Practical applications at the regional or national scale require many evaluations of the crop and/or observational operator models, particularly in the context of DA with iterative or sampling approaches. Most crop growth models take simulation units as independent of each other, and few simulate e.g. lateral flows of fluxes, which suggests that a parallel approach where different units can be spread out to different workers, is a feasible approach that can be successfully implemented in standard cloud architectures.

A different approach is to simplify the computational requirements of the crop and/or observation models. Rather than using the given model, approximations to the model can be used instead. In Gómez-Dans et al. (2016), the observation operators is approximated by an *emulator*: a proxy to the original model developed by using Gaussian Processes (GPs, see Camps-Valls et al., 2016 for a review of GPs in Earth Observation). The emulator not only is several orders of magnitude faster than the original model, but also provides access to the Jacobian and Hessian of the emulated model with minimal computational cost. This allows the implementation of efficient variational methods, as well as efficient MCMC methods that exploit gradient information in their proposal distribution. GPs have been successfully used to emulate many of the typical observation operators found in the literature, although their use by the crop growth modelling community has been very limited.

Current advances in SMP (symmetric multi-processor), GPU (graphical processing units) and computer clusters have resulted in standard software libraries that can form the building blocks of the general algorithms presented in Section 3. It is worth noting that developing software to fully exploit the capabilities of these massively parallel architectures is often hard, and not all problems are amenable to this treatment. Even if some authors (e.g. Lee et al., 2010) have raised

concerns casting doubt on some of the speed claims made for GPUs, these architectures have a potential to scale DA problems. In this context, the use of standard models through emulation can simplify their use: only the emulator code needs to be made efficient for the target architecture, a much simpler task than re-implementing crop or radiative transfer models for GPUs.

Going forward into the future, the use of massive parallel infrastructure, where the computing power as well as the data storage is available (systems similar to Google Earth Engine (GEE) (Gorelick et al., 2017), for example) might result in most of the DA problems being re-implemented to work on these system. For example, a Scalable satellite-based Crop Yield Mapper (SCYM) was developed (Lobell et al., 2015) to map crop yields with satellite data by using crop model simulations to train statistical models for different combinations of possible image acquisition dates, and then these models were applied to remote sensing images and gridded weather data within the GEE platform. However, the uncertainty of crop growth models is not considered by SCYM which differs itself from DA. The aforementioned approaches to modify problems described in the previous paragraphs will still apply directly to these architectures.

5.3. Advances in crop growth models

Generally, we need the crop growth model to dynamically simulate crop phenology, leaf area index, biomass, water use and grain yield formation in response to variations in genotype, environment and management, as well as their interactions (de Wit et al., 2015; He et al., 2017). A large number of crop growth models, such as APSIM (Keating et al., 2003), AquaCrop (Hsiao et al., 2009), CERES (Jones et al., 2003), GLAM (Challinor et al., 2004; Osborne et al., 2015), STICS (Brisson et al., 2003), SWAP (Eitzinger et al., 2004), WOFOST (Van Diepen et al., 1989), etc., have been used to predict crop growth and development under various environments during the last several decades. However, significant differences existed in model structures and parameters due to different aims and environments of model development (Wang et al., 2015; Ruane et al., 2016). Furthermore, crop growth models need to be improved to embed the latest progress in crop physiological processes and quantify the modeling uncertainty (Rötter et al., 2011). Fortunately, a part of these works is undertaken in the Agricultural Model Intercomparison and Improvement Project (AgMIP) (Rosenzweig et al., 2013). Within AgMIP a large number of crop and agronomy modelling groups cooperate to compare modelling results for existing crop datasets and for future conditions, including climate change. A similar idea, comparison of different RS-crop model DA based on the same dataset (remote sensing data and field data) are also suggested.

We can envisage a system where the different strengths of different models are pooled to provide an improved cropland monitoring capability, one where more observations allow for a better parameterisation of the interactions between crop growth, soil, weather, water, nutrients and management practices. Some progress in this direction has been made by using ensembles of models (Martre et al., 2015; Ruane et al., 2016), although a lot of work is still required.

A different approach can be taken in the light that the richness of observations that are currently available from satellites as well as from international *in situ* networks (Fang et al., 2014) might offer a large amount of information to the use of simpler crop growth models that are made to track a varied set of observations are of interest. For example, Revill et al. (2013) simplified the SPA-crop model of Sus et al. (2010) so as to provide a very simple crop growth model that is specifically designed to be used within DA frameworks to estimate the carbon balance of croplands: the simple model is designed to provide a general trajectory that is refined by assimilating a rich set of observations.

Most previous DA studies were performed based on crop growth models under potential condition, which implicitly simulate abiotic stress, as they all use meteorological variables as input, but these models may not simulate particular extreme events (e.g. frost kill on winter cereals, lodging) or biotic stress. Crop growth model under potential condition does not mean they are running under potential growth conditions. Taking flooding as example, it may happen, perhaps not often, and there are crop models (e.g. WOFOST) with a soil water balance that can roughly simulate the effect of flooding. Consequently, the existing DA studies take into account abiotic stress. Temporal variability of these parameters before and after the stress needs to be calibrated for improving the simulation of growth process. Improvement of simulation of crop growth model requires further calibration to account for the effect of water or temperature stress on dry matter accumulation during subsequent growth periods. When stress occurs, several key crop parameters of the crop growth model (e.g. the leaf CO_2 assimilation rate, conversion efficiency of assimilates, and partitioning parameters in WOFOST model) need to be calibrated based on the extent and duration of the historical stress in order to further improve the simulation accuracy of crop growth models.

6. Conclusion

In this paper, we have provided a systematic review of data assimilation (DA) in the field of crop modelling. We have provided a common framework to most of the DA literature by basing most methods in a Bayesian approach, where the different methods are presented as a set of different choices and assumptions in the goal of establishing a *a posteriori* pdf that combines a prior information (which in some cases can be the crop growth model) and a set of observations (often derived from satellite products).

The successful use of DA for crop monitoring results from the ability of observations to correct the evolution of the crop as modelled by imperfect crop growth models. A good example of the application of DA is the paper of Kang and Özdoğan (2019), where an initial coarse scale calibration of a crop model is performed first at the county level (e.g. coarse resolution), to then be refined at the Landsat pixel (30 m) level by assimilating Landsat observations. A less succesful study from Novelli and Vuolo (2019) in terms of yield estimation suggests that careful calibration of the model is critical to obtain sensible results from DA set ups. However, improving the yield estimate through assimilating high or medium resolution in the fragmented landscapes still remains a challenge (Huang et al., 2019; Defourny et al., 2019).

There are however a number of challenges ahead. Some of these stem from the observations, with strong requirements to combine observations from different sensors in a seamless way, and critically, provide accurate estimates of the uncertainty of the retrieved parameters. Part of this problem is inherent in the nature of satellite products, although recent advent of the Copernicus Sentinels satellites is changing the opportunities dramatically, making frequent high spatial resolution data (10 m resolut ion) available. Other challenges include the scaling of DA approaches to regional and national scales, where heterogeneity of croplands poses a challenge for models and improvements on the models to allow for more detailed processes, as well as advances to better understand the uncertainties in the modelling frameworks.

The increased spatial resolution, and the increasing simulated detail within crop models are challenging when facing large area operational applications. A number of strategies have been outlined, which include the use of surrogate modelling (emulators), as well as the use of efficient, massively parallel computational infrastructures.

Near real time applications, such as within-season forecasts are now possible thanks to the routine production of seasonal forecasts by weather centres across the world. While this area is still in its infancy, the use of seasonal forecasts coupled with DA approaches has a great promise in providing timely estimates of e.g. crop yield within the season, an important requirement for many agencies and users.

It is our firm belief that DA approaches will form the basis of future

crop monitoring systems. The fundamental limitations of crop models, meteorological drivers and EO data all suggest that a blend of all these realms is a necessity to provide a credible monitoring capability for croplands.

Acknowledgments

This study was supported by the National Natural Science Foundation of China (Project No. 41671418, 61661136006), and Fundamental Research Funds for the Chinese Central Universities (Project No. 2019TC117), and Science and Technology Facilities Council of UK-Newton Agritech Programme (Project No. ST/N006798/1), and NERC National Centre for Earth Observation (NCEO) (Project No. PR140015) and the European Commission H2020 MULTIPLY project (Project No. 687320).

References

Ades, M., van Leeuwen, P.J., 2013. An exploration of the equivalent weights particle filter. Q. J. R. Meteorol. Soc. 139 (April (672)), 820–840.
Ades, M., Van Leeuwen, P.J., 2015. The equivalent-weights particle filter in a high-dimensional system. Q. J. R. Meteorol. Soc. 141 (687), 484–503.
Anderson, B.D., Moore, J.B., 2012. Optimal Filtering. Courier Corporation.
Apipattanavis, S., Bert, F., Podestá, G., Rajagopalan, B., 2010. Linking weather generators and crop models for assessment of climate forecast outcomes. Agric. For. Meteorol. 150 (2), 166–174.
Arulampalam, M.S., Maskell, S., Gordon, N., Clapp, T., 2002. A tutorial on particle filters for online nonlinear/non-Gaussian Bayesian tracking. IEEE Trans. Signal Process. 50 (February (2)), 174–188.
Betbeder, J., Fieuzal, R., Baup, F., 2016. Assimilation of LAI and dry biomass data from optical and SAR images into an agro-meteorological model to estimate soybean yield. IEEE J. Sel. Top. Appl. Earth Obs. Remote Sens. 9 (6), 2540–2553.
Boogaard, H., De Wit, A., Te Roller, J., Van Diepen, C., 2014. WOFOST Control Centre 2.1; User's Guide for the WOFOST Control Centre 2.1 and the Crop Growth Simulation Model WOFOST 7.1.7. Alterra, Wageningen, The Netherlands.
Briers, M., Doucet, A., Maskell, S., 2009. Smoothing algorithms for state-space models. Ann. Inst. Stat. Math. 62 (June (1)), 61.
Brisson, N., Gary, C., Justes, E., Roche, R., Mary, B., Ripoche, D., Zimmer, D., Sierra, J., Bertuzzi, P., Burger, P., et al., 2003. An overview of the crop model stics. Eur. J. Agron. 18 (3–4), 309–332.
Burgers, G., Jan van Leeuwen, P., Evensen, G., 1998. Analysis scheme in the ensemble Kalman filter. Mon. Weather Rev. 126 (6), 1719–1724.
Camps-Valls, G., Verrelst, J., Munoz-Mari, J., Laparra, V., Mateo-Jimenez, F., Gomez-Dans, J., 2016. A survey on Gaussian processes for earth-observation data analysis: a comprehensive investigation. IEEE Geosci. Remote Sens. Mag. 4 (June (2)), 58–78.
Carton, J.A., Giese, B.S., 2008. A reanalysis of ocean climate using simple ocean data assimilation (SODA). Mon. Weather Rev. 136 (8), 2999–3017.
Ceglar, A., Črepinšek, Z., Kajfež-Bogataj, L., Pogačar, T., 2011. The simulation of phenological development in dynamic crop model: the Bayesian comparison of different methods. Agric. For. Meteorol. 151 (January (1)), 101–115.
Chakrabarti, S., Bongiovanni, T., Judge, J., Zotarelli, L., Bayer, C., 2014. Assimilation of smos soil moisture for quantifying drought impacts on crop yield in agricultural regions. IEEE J. Sel. Top. Appl. Earth Obs. Remote Sens. 7 (9), 3867–3879.
Challinor, A.J., Wheeler, T.R., Craufurd, P.Q., Slingo, J.M., Grimes, D.I.F., 2004. Design and optimisation of a large-area process-based model for annual crops. Agric. For. Meteorol. 124 (July (1)), 99–120.
Chaparro, D., Piles, M., Vall-Llossera, M., Camps, A., Konings, A.G., Entekhabi, D., 2018. L-band vegetation optical depth seasonal metrics for crop yield assessment. Remote Sens. Environ. 212, 249–259.
Charney, J., Halem, M., Jastrow, R., 1969. Use of incomplete historical data to infer the present state of the atmosphere. J. Atmos. Sci. 26 (5), 1160–1163.
Chen, J.M., 1999. Spatial scaling of a remotely sensed surface parameter by contexture – three land-atmospheric modeling experiments. Remote Sens. Environ. 69 (1), 30–42.
Chen, Y., Cournède, P.-H., 2014. Data assimilation to reduce uncertainty of crop model prediction with convolution particle filtering. Ecol. Model. 290, 165–177.
Chen, Y., Zhang, Z., Tao, F., 2018. Improving regional winter wheat yield estimation through assimilation of phenology and leaf area index from remote sensing data. Eur. J. Agron. 101, 163–173.
Cheng, Z., Meng, J., Qiao, Y., Wang, Y., Dong, W., Han, Y., 2018. Preliminary study of soil available nutrient simulation using a modified WOFOST model and time-series remote sensing observations. Remote Sens. 10 (1), 64.
Claverie, M., Ju, J., Masek, J.G., Dungan, J.L., Vermote, E.F., Roger, J.-C., Skakun, S.V., Justice, C., 2018. The Harmonized Landsat and Sentinel-2 surface reflectance data set. Remote Sens. Environ. 219 (December), 145–161.
Courtier, P., Thépaut, J.-N., Hollingsworth, A., 1994. A strategy for operational implementation of 4D-Var, using an incremental approach. Q. J. R. Meteorol. Soc. 120 (519), 1367–1387.
Cowles, M.K., Carlin, B.P., 1996. Markov chain Monte Carlo convergence diagnostics: a comparative review. J. Am. Stat. Assoc. 91 (June (434)), 883–904.
Croft, H., Chen, J.M., Luo, X., Bartlett, P., Chen, B., Staebler, R.M., 2017. Leaf chlorophyll content as a proxy for leaf photosynthetic capacity. Glob. Change Biol. 23 (9), 3513–3524.
Curnel, Y., de Wit, A.J., Duveiller, G., Defourny, P., 2011. Potential performances of remotely sensed LAI assimilation in WOFOST model based on an OSS experiment. Agric. For. Meteorol. 151 (12), 1843–1855.
de Wit, A., Boogaard, H., van Diepen, K., van Kraalingen, D., Rötter, R., Supit, I., Wolf, J., van Ittersum, M., 2015. WOFOST developer's response to article by Stella et al., Environmental Modelling & Software 59 (2014). Environ. Model. Softw. 73 (C), 57–59.
de Wit, A., Duveiller, G., Defourny, P., 2012. Estimating regional winter wheat yield with WOFOST through the assimilation of green area index retrieved from MODIS observations. Agric. For. Meteorol. 164, 39–52.
de Wit, A.J.W., van Diepen, C.A., 2007a. Crop model data assimilation with the Ensemble Kalman filter for improving regional crop yield forecasts. Agric. For. Meteorol. 146 (September (1–2)), 38–56.
de Wit, A.J.W., van Diepen, C.A., 2007b. Crop model data assimilation with the ensemble Kalman filter for improving regional crop yield forecasts. Agric. For. Meteorol. 146 (1–2), 38–56.
Dee, D.P., Uppala, S.M., Simmons, A., Berrisford, P., Poli, P., Kobayashi, S., Andrae, U., Balmaseda, M., Balsamo, G., Bauer, d.P., et al., 2011. The ERA-interim reanalysis: configuration and performance of the data assimilation system. Q. J. R. Meteorol. Soc. 137 (656), 553–597.
Defourny, P., Bontemps, S., Bellemans, N., Cara, C., Dedieu, G., Guzzonato, E., ... Koetz, B., 2019. Near real-time agriculture monitoring at national scale at parcel resolution: performance assessment of the Sen2-Agri automated system in various cropping systems around the world. Remote Sens. Environ. 221, 551–568. https://doi.org/10.1016/j.rse.2018.11.007.
Delécolle, R., Maas, S., Guérif, M., Baret, F., 1992. Remote sensing and crop production models: present trends. ISPRS J. Photogramm. Remote Sens. 47 (2–3), 145–161.
Delloye, C., Weiss, M., Defourny, P., 2018. Retrieval of the canopy chlorophyll content from Sentinel-2 spectral bands to estimate nitrogen uptake in intensive winter wheat cropping systems. Remote Sens. Environ. 216 (October), 245–261.
Dente, L., Satalino, G., Mattia, F., Rinaldi, M., 2008. Assimilation of leaf area index derived from ASAR and MERIS data into CERES-wheat model to map wheat yield. Remote Sens. Environ. 112 (4), 1395–1407.
Doblas-Reyes, F.J., Garc’í-Serrano, J., Lienert, F., Biescas, A.P., Rodrigues, L.R.L., 2013. Seasonal climate predictability and forecasting: status and prospects. Wiley Interdiscip. Rev.: Clim. Change 4 (July (4)), 245–268.
Dong, T., Liu, J., Qian, B., Zhao, T., Jing, Q., Geng, X., Wang, J., Huffman, T., Shang, J., 2016. Estimating winter wheat biomass by assimilating leaf area index derived from fusion of Landsat-8 and MODIS data. Int. J. Appl. Earth Obs. Geoinf. 49, 63–74.
Dong, Y., Wang, J., Li, C., Yang, G., Wang, Q., Liu, F., Zhao, J., Wang, H., Huang, W., 2013. Comparison and analysis of data assimilation algorithms for predicting the leaf area index of crop canopies. IEEE J. Sel. Top. Appl. Earth Obs. Remote Sens. 6 (1), 188–201.
Dorigo, W., Wagner, W., Albergel, C., Albrecht, F., Balsamo, G., Brocca, L., Chung, D., Ertl, M., Forkel, M., Gruber, A., et al., 2017. ESA CCI soil moisture for improved earth system understanding: state-of-the art and future directions. Remote Sens. Environ. 203, 185–215.
Dorigo, W.A., Zurita-Milla, R., de Wit, A.J., Brazile, J., Singh, R., Schaepman, M.E., 2007. A review on reflective remote sensing and data assimilation techniques for enhanced agroecosystem modeling. Int. J. Appl. Earth Obs. Geoinf. 9 (2), 165–193.
Dowd, M., 2006. A sequential Monte Carlo approach for marine ecological prediction. Environmetrics 17 (August (5)), 435–455.
Dowd, M., 2007. Bayesian statistical data assimilation for ecosystem models using Markov Chain Monte Carlo. J. Mar. Syst. 68 (December (3–4)), 439–456.
Dumont, B., Leemans, V., Mansouri, M., Bodson, B., Destain, J.-P., Destain, M.-F., 2014. Parameter identification of the STICS crop model, using an accelerated formal MCMC approach. Environ. Model. Softw. 52 (February), 121–135.
Duveiller, G., Lopez-Lozano, R., Cescatti, A., 2015. Exploiting the multi-angularity of the MODIS temporal signal to identify spatially homogeneous vegetation cover: a demonstration for agricultural monitoring applications. Remote Sens. Environ. 166, 61–77.
Duveiller, G., Weiss, M., Baret, F., Defourny, P., 2011. Retrieving wheat green area index during the growing season from optical time series measurements based on neural network radiative transfer inversion. Remote Sens. Environ. 115 (3), 887–896.
Eitzinger, J., Trnka, M., Hösch, J., Žalud, Z., Dubrovský, M., 2004. Comparison of CERES, WOFOST and SWAP models in simulating soil water content during growing season under different soil conditions. Ecol. Model. 171 (3), 223–246.
Evensen, G., 1994. Sequential data assimilation with a nonlinear quasi-geostrophic model using Monte Carlo methods to forecast error statistics. J. Geophys. Res.: Oceans 99 (C5), 10143–10162.
Evensen, G., 2003. The Ensemble Kalman Filter: theoretical formulation and practical implementation. Ocean Dyn. 53 (4), 343–367.
Fang, H., Liang, S., Hoogenboom, G., 2011. Integration of MODIS LAI and vegetation index products with the CSM-CERES-MAIZE model for corn yield estimation. Int. J. Remote Sens. 32 (4), 1039–1065.
Fang, H., Liang, S., Hoogenboom, G., Teasdale, J., Cavigelli, M., 2008. Corn-yield estimation through assimilation of remotely sensed data into the CSM-CERES-MAIZE model. Int. J. Remote Sens. 29 (10), 3011–3032.
Fang, S., Xu, L.D., Zhu, Y., Ahati, J., Pei, H., Yan, J., Liu, Z., 2014. An integrated system for regional environmental monitoring and management based on Internet of things. IEEE Trans. Ind. Inform. 10 (May (2)), 1596–1605.
FAO, 2017. The Future of Food and Agriculture-Trends and Challenges.
Fisher, M., Leutbecher, M., Kelly, G.A., 2005. On the equivalence between Kalman smoothing and weak-constraint four-dimensional variational data assimilation. Q. J.

R. Meteorol. Soc. 131 (613), 3235–3246.
Fitzgerald, R., 1971. Divergence of the Kalman filter. IEEE Trans. Autom. Control 16 (December (6)), 736–747.
Gao, Q., Yu, M., Yang, X., Wu, J., 2001. Scaling simulation models for spatially heterogeneous ecosystems with diffusive transportation. Landsc. Ecol. 16 (4), 289–300.
Garrigues, S., Allard, D., Baret, F., Weiss, M., 2006. Influence of landscape spatial heterogeneity on the non-linear estimation of leaf area index from moderate spatial resolution remote sensing data. Remote Sens. Environ. 105 (4), 286–298.
Gelman, A., Carlin, J.B., Stern, H.S., Dunson, D.B., Vehtari, A., Rubin, D.B., 2013. Bayesian Data Analysis. CRC Press.
Giering, R., Kaminski, T., 1998. Recipes for adjoint code construction. ACM Trans. Math. Softw. 24 (December (4)), 437–474.
Gilks, W.R., Richardson, S., Spiegelhalter, D., December 1995. Markov chain Monte Carlo in Practice. CRC Press.
Giorgi, F., Jones, C., Asrar, G.R., et al., 2009. Addressing climate information needs at the regional level: the CORDEX framework. World Meteorol. Organ. (WMO) Bull. 58 (3), 175.
Gitelson, A.A., Viña, A., Verma, S.B., Rundquist, D.C., Arkebauer, T.J., Keydan, G., Leavitt, B., Ciganda, V., Burba, G.G., Suyker, A.E., 2006. Relationship between gross primary production and chlorophyll content in crops: implications for the synoptic monitoring of vegetation productivity. J. Geophys. Res. 111 (D8), 168.
Gómez-Dans, J., Lewis, P., Disney, M., 2016. Efficient emulation of radiative transfer codes using Gaussian processes and application to land surface parameter inferences. Remote Sens. 8 (February (2)), 119.
Gorelick, N., Hancher, M., Dixon, M., Ilyushchenko, S., Thau, D., Moore, R., 2017. Google earth engine: planetary-scale geospatial analysis for everyone. Remote Sens. Environ. 202, 18–27.
Guan, K., Berry, J.A., Zhang, Y., Joiner, J., Guanter, L., Badgley, G., Lobell, D.B., 2016. Improving the monitoring of crop productivity using spaceborne solar-induced fluorescence. Glob. Change Biol. 22 (2), 716–726.
Guanter, L., Frankenberg, C., Dudhia, A., Lewis, P.E., Gómez-Dans, J., Kuze, A., Suto, H., Grainger, R.G., 2012. Retrieval and global assessment of terrestrial chlorophyll fluorescence from GOSAT space measurements. Remote Sens. Environ. 121, 236–251.
Guanter, L., Zhang, Y., Jung, M., Joiner, J., Voigt, M., Berry, J.A., Frankenberg, C., Huete, A.R., Zarco-Tejada, P., Lee, J.-E., Moran, M.S., Ponce-Campos, G., Beer, C., Camps-Valls, G., Buchmann, N., Gianelle, D., Klumpp, K., Cescatti, A., Baker, J.M., Griffis, T.J., 2014. Global and time-resolved monitoring of crop photosynthesis with chlorophyll fluorescence. Proc. Natl. Acad. Sci. U. S. A. 111 (April (14)), E1327–33.
Guérif, M., Duke, C., 1998. Calibration of the sucros emergence and early growth module for sugar beet using optical remote sensing data assimilation. Eur. J. Agron. 9 (2–3), 127–136.
Guerif, M., Duke, C., 2000. Adjustment procedures of a crop model to the site specific characteristics of soil and crop using remote sensing data assimilation. Agric. Ecosyst. Environ. 81 (1), 57–69.
Guo, C., Zhang, L., Zhou, X., Zhu, Y., Cao, W., Qiu, X., Cheng, T., Tian, Y., 2018. Integrating remote sensing information with crop model to monitor wheat growth and yield based on simulation zone partitioning. Precis. Agric. 19 (1), 55–78.
Hank, T., Bach, H., Mauser, W., 2015. Using a remote sensing-supported hydro-agroecological model for field-scale simulation of heterogeneous crop growth and yield: application for wheat in Central Europe. Remote Sens. 7 (April (4)), 3934–3965.
Hansen, J.W., Challinor, A., Ines, A.V.M., Wheeler, T., Moron, V., 2006. Translating climate forecasts into agricultural terms: advances and challenges. Clim. Res. 33 (1), 27–41.
Hansen, J.W., Jones, J.W., 2000. Scaling-up crop models for climate variability applications. Agric. Syst. 65 (1), 43–72.
Hartig, F., Calabrese, J.M., Reineking, B., Wiegand, T., Huth, A., 2011. Statistical inference for stochastic simulation models – theory and application. Ecol. Lett. 14 (8), 816–827.
He, B., Li, X., Quan, X., Qiu, S., 2015. Estimating the aboveground dry biomass of grass by assimilation of retrieved LAI into a crop growth model. IEEE J. Sel. Top. Appl. Earth Obs. Remote Sens. 8 (2), 550–561.
He, D., Wang, E., Wang, J., Lilley, J.M., 2017. Genotype × environment × management interactions of canola across China: a simulation study. Agric. For. Meteorol. 247, 424–433.
Hoefsloot, P., Ines, A.V., van Dam, J., Duveiller, G., Kayitakire, F., Hansen, J., 2012. Combining Crop Models and Remote Sensing for Yield Prediction: Concepts, Applications and Challenges for Heterogeneous Smallholder Environments. Publications Office of the European Union, Luxembourg.
Holzworth, D.P., Snow, V., Janssen, S., Athanasiadis, I.N., Donatelli, M., Hoogenboom, G., White, J.W., Thorburn, P., 2015. Agricultural production systems modelling and software: current status and future prospects. Environ. Model. Softw. 72, 276–286.
Hoogenboom, G., 2000. Contribution of agrometeorology to the simulation of crop production and its applications. Agric. For. Meteorol. 103 (1–2), 137–157.
Hsiao, T.C., Heng, L., Steduto, P., Rojas-Lara, B., Raes, D., Fereres, E., 2009. Aquacrop – the FAO crop model to simulate yield response to water: III. Parameterization and testing for maize. Agron. J. 101 (3), 448–459.
Hu, T., Su, Y., Xue, B., Liu, J., Zhao, X., Fang, J., Guo, Q., 2016. Mapping global forest aboveground biomass with spaceborne lidar, optical imagery, and forest inventory data. Remote Sens. 8 (7), 565.
Huang, J., Ma, H., Sedano, F., Lewis, P., Liang, S., Wu, Q., Su, W., Zhang, X., Zhu, D., 2019. Evaluation of regional estimates of winter wheat yield by assimilating three remotely sensed reflectance datasets into the coupled WOFOST-prosail model. Eur. J. Agron. 102, 1–13.
Huang, J., Ma, H., Su, W., Zhang, X., Huang, Y., Fan, J., Wu, W., 2015a. Jointly assimilating MODIS LAI and ET products into the SWAP model for winter wheat yield estimation. IEEE J. Sel. Top. Appl. Earth Obs. Remote Sens. 8 (8), 4060–4071.
Huang, J., Tian, L., Liang, S., Ma, H., Becker-Reshef, I., Huang, Y., Su, W., Zhang, X., Zhu, D., Wu, W., 2015b. Improving winter wheat yield estimation by assimilation of the leaf area index from Landsat TM and MODIS data into the WOFOST model. Agric. For. Meteorol. 204, 106–121.
Huang, J., Sedano, F., Huang, Y., Ma, H., Li, X., Liang, S., Tian, L., Zhang, X., Fan, J., Wu, W., 2016. Assimilating a synthetic Kalman filter leaf area index series into the WOFOST model to improve regional winter wheat yield estimation. Agric. For. Meteorol. 216, 188–202.
Huang, Y., Zhu, Y., Li, W., Cao, W., Tian, Y., 2013. Assimilating remotely sensed information with the wheatgrow model based on the ensemble square root filter for improving regional wheat yield forecasts. Plant Prod. Sci. 16 (4), 352–364.
Iizumi, T., Yokozawa, M., Nishimori, M., 2009. Parameter estimation and uncertainty analysis of a large-scale crop model for paddy rice: application of a Bayesian approach. Agric. For. Meteorol. 149 (February (2)), 333–348.
Ines, A.V., Honda, K., Gupta, A.D., Droogers, P., Clemente, R.S., 2006. Combining remote sensing-simulation modeling and genetic algorithm optimization to explore water management options in irrigated agriculture. Agric. Water Manag. 83 (3), 221–232.
Ines, A.V.M., Das, N.N., Hansen, J.W., Njoku, E.G., 2013. Assimilation of remotely sensed soil moisture and vegetation with a crop simulation model for maize yield prediction. Remote Sens. Environ. 138, 149–164.
Inoue, Y., Kurosu, T., Maeno, H., Uratsuka, S., Kozu, T., Dabrowska-Zielinska, K., Qi, J., 2002. Season-long daily measurements of multifrequency (Ka, Ku, X, C, and L) and full-polarization backscatter signatures over paddy rice field and their relationship with biological variables. Remote Sens. Environ. 81 (2–3), 194–204.
IPCC, 2018. Summary for policymakers. In: Masson-Delmotte, V., Zhai, P., Pörtner, H.-O., Roberts, D., Skea, J., Shukla, P., Pirani, A., Moufouma-Okia, W., Péan, C., Pidcock, R., Connors, S., Matthews, J., Chen, Y., Zhou, X., Gomis, M., Lonnoy, E., Maycock, T., Tignor, M., Waterfield, T. (Eds.), Global Warming of 1.5 °C. An IPCC Special Report on the impacts of global warming of 1.5 °C above pre-industrial levels and related global greenhouse gas emission pathways, in the context of strengthening the global response to the threat of climate change, sustainable development, and efforts to eradicate poverty. World Meteorological Organization, Geneva, Switzerland 32 pp.
Jazwinski, A.H., 2007. Stochastic Processes and Filtering Theory. Courier Corporation.
Jégo, G., Pattey, E., Liu, J., 2012. Using leaf area index, retrieved from optical imagery, in the stics crop model for predicting yield and biomass of field crops. Field Crops Res. 131 (2), 63–74.
Jiang, J., Ji, X., Yao, X., Tian, Y., Zhu, Y., Cao, W., Cheng, T., 2018. Evaluation of three techniques for correcting the spatial scaling bias of leaf area index. Remote Sens. 10 (2), 221.
Jiang, Z., Chen, Z., Chen, J., Liu, J., Ren, J., Li, Z., Sun, L., Li, H., 2014. Application of crop model data assimilation with a particle filter for estimating regional winter wheat yields. IEEE J. Sel. Top. Appl. Earth Obs. Remote Sens. 7 (11), 4422–4431.
Jin, H., Li, A., Wang, J., Bo, Y., 2016. Improvement of spatially and temporally continuous crop leaf area index by integration of CERES-maize model and MODIS data. Eur. J. Agron. 78, 1–12.
Jin, M., Liu, X., Wu, L., Liu, M., 2015. An improved assimilation method with stress factors incorporated in the WOFOST model for the efficient assessment of heavy metal stress levels in rice. Int. J. Appl. Earth Obs. Geoinf. 41, 118–129.
Jin, X., Kumar, L., Li, Z., Feng, H., Xu, X., Yang, G., Wang, J., 2018. A review of data assimilation of remote sensing and crop models. Eur. J. Agron. 92.
Jin, X., Li, Z., Yang, G., Yang, H., Feng, H., Xu, X., Wang, J., Li, X., Luo, J., 2017. Winter wheat yield estimation based on multi-source medium resolution optical and radar imaging data and the AquaCrop model using the particle swarm optimization algorithm. ISPRS J. Photogramm. Remote Sens. 126, 24–37.
Joiner, J., Yoshida, Y., Vasilkov, A., Middleton, E., et al., 2011. First observations of global and seasonal terrestrial chlorophyll fluorescence from space. Biogeosciences 8 (3), 637–651.
Jones, J.W., Hoogenboom, G., Porter, C.H., Boote, K.J., Batchelor, W.D., Hunt, L., Wilkens, P.W., Singh, U., Gijsman, A.J., Ritchie, J.T., 2003. The dssat cropping system model. Eur. J. Agron. 18 (3–4), 235–265.
Kaminski, T., Pinty, B., Voßbeck, M., Lopatka, M., Gobron, N., Robustelli, M., 2017. Consistent retrieval of land surface radiation products from EO, including traceable uncertainty estimates. Biogeosciences 14 (May (9)), 2527–2541.
Kang, Y., Özdoğan, M., 2019. Field-level crop yield mapping with landsat using a hierarchical data assimilation approach. Remote Sens. Environ. 228, 144–163.
Kasampalis, D., Alexandridis, T., Deva, C., Challinor, A., Moshou, D., Zalidis, G., 2018. Contribution of remote sensing on crop models: a review. J. Imaging 4 (4), 52.
Keating, B.A., Carberry, P.S., Hammer, G.L., Probert, M.E., Robertson, M.J., Holzworth, D., Huth, N.I., Hargreaves, J.N., Meinke, H., Hochman, Z., et al., 2003. An overview of apsim, a model designed for farming systems simulation. Eur. J. Agron. 18 (3–4), 267–288.
Kerr, Y.H., Waldteufel, P., Wigneron, J., Delwart, S., Cabot, F., Boutin, J., Escorihuela, M., Font, J., Reul, N., Gruhier, C., Juglea, S.E., Drinkwater, M.R., Hahne, A., Martin-Neira, M., Mecklenburg, S., 2010. The SMOS mission: new tool for monitoring key elements of the global water cycle. Proc. IEEE 98 (May (5)), 666–687.
Knyazikhin, Y., Martonchik, J.V., Myneni, R.B., Diner, D.J., Running, S.W., 1998. Synergistic algorithm for estimating vegetation canopy leaf area index and fraction of absorbed photosynthetically active radiation from MODIS and MISR data. J. Geophys. Res. 103 (D24), 32257–32275.
Launay, M., Guerif, M., 2005. Assimilating remote sensing data into a crop model to improve predictive performance for spatial applications. Agric. Ecosyst. Environ. 111 (1–4), 321–339.
Laurent, V.C.E., Schaepman, M.E., Verhoef, W., Weyermann, J., Chávez, R.O., 2014. Bayesian object-based estimation of LAI and chlorophyll from a simulated Sentinel-2 top-of-atmosphere radiance image. Remote Sens. Environ. 140 (January), 318–329.
Laurent, V.C.E., Verhoef, W., Damm, A., Schaepman, M.E., Clevers, J.G.P.W., 2013. A

Bayesian object-based approach for estimating vegetation biophysical and biochemical variables from APEX at-sensor radiance data. Remote Sens. Environ. 139 (December), 6–17.
Lawless, C., Semenov, M.A., 2005. Assessing lead-time for predicting wheat growth using a crop simulation model. Agric. For. Meteorol. 135 (December (1)), 302–313.
Le Dimet, F.-X., Talagrand, O., 1986. Variational algorithms for analysis and assimilation of meteorological observations: theoretical aspects. Tellus Ser. A: Dyn. Meteorol. Oceanogr. 38 (January (2)), 97–110.
Lee, P.M., 2012. Bayesian Statistics: An Introduction. Wiley.
Lee, V.W., Kim, C., Chhugani, J., Deisher, M., Kim, D., Nguyen, A.D., Satish, N., Smelyanskiy, M., Chennupaty, S., Hammarlund, P., Singhal, R., Dubey, P., 2010. Debunking the 100X GPU vs. CPU myth: an evaluation of throughput computing on CPU and GPU. SIGARCH Comput. Archit. News 38 (June (3)), 451–460.
Lehuger, S., Gabrielle, B., van Oijen, M., Makowski, D., Germon, J.-C., Morvan, T., Hénault, C., 2009. Bayesian calibration of the nitrous oxide emission module of an agro-ecosystem model. Agric. Ecosyst. Environ. 133 (October (3)), 208–222.
Lewis, P., Gómez-Dans, J., Kaminski, T., Settle, J., Quaife, T., Gobron, N., Styles, J., Berger, M., 2012. An earth observation land data assimilation system (EO-LDAS). Remote Sens. Environ. 120 (120), 219–235.
Li, X., Wang, J., Strahler, A.H., 1999. Scale effect of Planck's law over nonisothermal blackbody surface. Sci. China 42 (6), 652–656.
Li, Y., Zhou, Q., Zhou, J., Zhang, G., Chen, C., Wang, J., 2014. Assimilating remote sensing information into a coupled hydrology-crop growth model to estimate regional maize yield in arid regions. Ecol. Model. 291, 15–27.
Li, Z., Wang, J., Xu, X., Zhao, C., Jin, X., Yang, G., Feng, H., 2015. Assimilation of two variables derived from hyperspectral data into the DSSAT-CERES model for grain yield and quality estimation. Remote Sens. 7 (9), 12400–12418.
Liang, S., 2000. Numerical experiments on the spatial scaling of land surface albedo and leaf area index. Remote Sens. Rev. 19 (December (1–4)), 225–242.
Liang, S., 2004. Quantitative Remote Sensing of Land Surfaces, vol. 1 Wiley & Sons, Hoboken, etc.
Liang, S., Qin, J., 2008. Data assimilation methods for land surface variable estimation. Advances in Land Remote Sensing. Springer, pp. 313–339.
Ließ, M., Glaser, B., Huwe, B., 2012. Uncertainty in the spatial prediction of soil texture: comparison of regression tree and Random Forest models. Geoderma 170 (January), 70–79.
Lin, C., Wang, Z., Zhu, J., 2008. An ensemble Kalman filter for severe dust storm data assimilation over China. Atmos. Chem. Phys. 8 (11), 2975–2983.
Liu, F., Liu, X., Ding, C., Wu, L., 2015. The dynamic simulation of rice growth parameters under cadmium stress with the assimilation of multi-period spectral indices and crop model. Field Crops Res. 183, 225–234.
Liu, Y.Y., Dorigo, W.A., Parinussa, R., de Jeu, R.A., Wagner, W., McCabe, M.F., Evans, J., Van Dijk, A., 2012. Trend-preserving blending of passive and active microwave soil moisture retrievals. Remote Sens. Environ. 123, 280–297.
Lobell, D.B., Thau, D., Seifert, C., Engle, E., Little, B., 2015. A scalable satellite-based crop yield mapper. Remote Sens. Environ. 164, 324–333.
Lorenc, A.C., 1986. Analysis methods for numerical weather prediction. Q. J. R. Meteorol. Soc. 112 (October (474)), 1177–1194.
Lv, Z., Liu, X., Cao, W., Zhu, Y., 2013. Climate change impacts on regional winter wheat production in main wheat production regions of China. Agric. For. Meteorol. 171, 234–248.
Ma, G., Huang, J., Wu, W., Fan, J., Zou, J., Wu, S., 2013a. Assimilation of MODIS-LAI into the WOFOST model for forecasting regional winter wheat yield. Math. Comput. Model. 58 (3–4), 634–643.
Ma, H., Huang, J., Zhu, D., Liu, J., Su, W., Zhang, C., Fan, J., 2013b. Estimating regional winter wheat yield by assimilation of time series of HJ-1 CCD NDVI into WOFOST ACRM model with ensemble Kalman filter. Math. Comput. Model. 58 (3–4), 753–764.
Ma, Y., Wang, S., Zhang, L., Hou, Y., Zhuang, L., He, Y., Wang, F., 2008. Monitoring winter wheat growth in North China by combining a crop model and remote sensing data. Int. J. Appl. Earth Obs. Geoinf. 10 (4), 426–437.
Maas, S.J., 1988. Use of remotely-sensed information in agricultural crop growth models. Ecol. Model. 41 (3–4), 247–268.
MacBean, N., Maignan, F., Bacour, C., Lewis, P., Peylin, P., Guanter, L., Köhler, P., Gómez-Dans, J., Disney, M., 2018. Author Correction: Strong constraint on modelled global carbon uptake using solar-induced chlorophyll fluorescence data. Sci. Rep. 8 (July (1)), 10420.
Machwitz, M., Giustarini, L., Bossung, C., Frantz, D., Schlerf, M., Lilienthal, H., Wandera, L., Matgen, P., Hoffmann, L., Udelhoven, T., 2014. Enhanced biomass prediction by assimilating satellite data into a crop growth model. Environ. Model. Softw. 62, 437–453.
Makowski, D., Wallach, D., Tremblay, M., 2002. Using a Bayesian approach to parameter estimation; comparison of the GLUE and MCMC methods. Agronomie 22 (2), 191–203.
Marin, F., Jones, J.W., Boote, K.J., 2017. A stochastic method for crop models: including uncertainty in a sugarcane model. Agron. J. 109 (2), 483–495.
Marletto, V., Ventura, F., Fontana, G., Tomei, F., 2007. Wheat growth simulation and yield prediction with seasonal forecasts and a numerical model. Agric. For. Meteorol. 147 (1), 71–79.
Martens, B., Gonzalez Miralles, D., Lievens, H., Van Der Schalie, R., De Jeu, R.A., Fernández-Prieto, D., Beck, H.E., Dorigo, W., Verhoest, N., 2017. GLEAM v3: satellite-based land evaporation and root-zone soil moisture. Geosci. Model Dev. 10 (5), 1903–1925.
Martínez, B., García-Haro, F.J., Coca, C.D., 2009. Derivation of high-resolution leaf area index maps in support of validation activities: application to the cropland barrax site. Agric. For. Meteorol. 149 (1), 130–145.
Martre, P., Wallach, D., Asseng, S., Ewert, F., Jones, J.W., Rötter, R.P., Boote, K.J., Ruane, A.C., Thorburn, P.J., Cammarano, D., 2015. Multimodel ensembles of wheat growth: many models are better than one. Glob. Change Biol. 21 (2), 911–925.
Matgen, P., Montanari, M., Hostache, R., Pfister, L., Hoffmann, L., Plaza, D., Pauwels, V., De Lannoy, G., De Keyser, R., Savenije, H., 2010. Towards the sequential assimilation of SAR-derived water stages into hydraulic models using the particle filter: proof of concept. Hydrol. Earth Syst. Sci. 14 (9), 1773–1785.
Merchant, C.J., Paul, F., Popp, T., Ablain, M., Bontemps, S., Defourny, P., Hollmann, R., Lavergne, T., Laeng, A., Leeuw, G.d., Mittaz, J., Poulsen, C., Povey, A.C., Reuter, M., Sathyendranath, S., Sandven, S., Sofieva, V.F., Wagner, W., 2017. Uncertainty information in climate data records from Earth observation. Earth Syst. Sci. Data 9 (July (2)), 511–527.
Meroni, M., Rossini, M., Guanter, L., Alonso, L., Rascher, U., Colombo, R., Moreno, J., 2009. Remote sensing of solar-induced chlorophyll fluorescence: review of methods and applications. Remote Sens. Environ. 113 (10), 2037–2051.
Meza, F.J., Hansen, J.W., Osgood, D., 2008. Economic value of seasonal climate forecasts for agriculture: review of ex-ante assessments and recommendations for future research. J. Appl. Meteorol. Climatol. 47 (May (5)), 1269–1286.
Miller, J.R., Chen, J.M., Rubinstein, I.G., 2004. Evaluating image-based estimates of leaf area index in boreal conifer stands over a range of scales using high-resolution CASI imagery. Remote Sens. Environ. 89 (2), 200–216.
Miralles, D., Holmes, T., De Jeu, R., Gash, J., Meesters, A., Dolman, A., et al., 2011. Global Land-Surface Evaporation Estimated from Satellite-Based Observations.
Mishra, A.K., Ines, A.V., Das, N.N., Khedun, C.P., Singh, V.P., Sivakumar, B., Hansen, J.W., 2015. Anatomy of a local-scale drought: application of assimilated remote sensing products, crop model, and statistical methods to an agricultural drought study. J. Hydrol. 526, 15–29.
Molijn, R.A., Iannini, L., Mousivand, A., Hanssen, R.F., 2014. Analyzing C-band SAR polarimetric information for LAI and crop yield estimations. Proc. SPIE – Int. Soc. Opt. Eng. 9239 92390V-92390V-11.
Montzka, C., Moradkhani, H., Weihermüller, L., Franssen, H.-J.H., Canty, M., Vereecken, H., 2011. Hydraulic parameter estimation by remotely-sensed top soil moisture observations with the particle filter. J. Hydrol. 399 (3–4), 410–421.
Moradkhani, H., DeChant, C.M., Sorooshian, S., 2012. Evolution of ensemble data assimilation for uncertainty quantification using the particle filter-Markov chain Monte Carlo method. Water Resour. Res. 48 (12).
Moradkhani, H., Hsu, K.-L., Gupta, H., Sorooshian, S., 2005. Uncertainty assessment of hydrologic model states and parameters: sequential data assimilation using the particle filter. Water Resour. Res. 41 (5).
Mousivand, A., Menenti, M., Gorte, B., Verhoef, W., 2015. Multi-temporal, multi-sensor retrieval of terrestrial vegetation properties from spectral-directional radiometric data. Remote Sens. Environ. 158 (March), 311–330.
Mu, Q., Heinsch, F.A., Zhao, M., Running, S.W., 2007. Development of a global evapotranspiration algorithm based on MODIS and global meteorology data. Remote Sens. Environ. 111 (4), 519–536.
Nearing, G.S., Crow, W.T., Thorp, K.R., Moran, M.S., Reichle, R.H., Gupta, H.V., 2012. Assimilating remote sensing observations of leaf area index and soil moisture for wheat yield estimates: an observing system simulation experiment. Water Resour. Res. 48 (5).
Njoku, E.G., Jackson, T.J., Lakshmi, V., Chan, T.K., Nghiem, S.V., 2003. Soil moisture retrieval from AMSR-E. IEEE Trans. Geosci. Remote Sens. 41 (February (2)), 215–229.
Norton, A.J., Rayner, P.J., Koffi, E.N., Scholze, M., 2018. Assimilating solar-induced chlorophyll fluorescence into the terrestrial biosphere model BETHY-SCOPE v1.0: model description and information content. Geosci. Model Dev. 11 (4), 1517–1536.
Novelli, F., Vuolo, F., 2019. Assimilation of sentinel-2 leaf area index data into a physically-based crop growth model for yield estimation. Agronomy 9 (5), 255. https://doi.org/10.3390/agronomy9050255.
Olioso, A., Chauki, H., Courault, D., Wigneron, J.-P., 1999. Estimation of evapotranspiration and photosynthesis by assimilation of remote sensing data into SVAT models. Remote Sens. Environ. 68 (June (3)), 341–356.
Olioso, A., Inoue, Y., Ortega-FARIA, S., Demarty, J., Wigneron, J.-P., Braud, I., Jacob, F., Lecharpentier, P., OttlÉ, C., Calvet, J.-C., Brisson, N., 2005. Future directions for advanced evapotranspiration modeling: assimilation of remote sensing data into crop simulation models and SVAT models. Irrig. Drain. Syst. 19 (November (3)), 377–412.
Osborne, T., Gornall, J., Hooker, J., Williams, K., Wiltshire, A., Betts, R., Wheeler, T., 2015. JULES-crop: a parametrisation of crops in the Joint UK Land Environment Simulator. Geosci. Model Dev. 8 (April (4)), 1139–1155.
Parker, W.S., 2016. Reanalyses and observations: what's the difference? Bull. Am. Meteorol. Soc. 97 (9), 1565–1572.
Patenaude, G., Milne, R., Van Oijen, M., Rowland, C., Hill, R., 2008. Integrating remote sensing datasets into ecological modelling: a Bayesian approach. Int. J. Remote Sens. 29 (5), 1295–1315.
Pauwels, V., Verhoest, N.E., De Lannoy, G.J., Guissard, V., Lucau, C., Defourny, P., 2007. Optimization of a coupled hydrology – crop growth model through the assimilation of observed soil moisture and leaf area index values using an ensemble Kalman filter. Water Resour. Res. 43 (4).
Poggio, L., Gimona, A., 2014. National scale 3D modelling of soil organic carbon stocks with uncertainty propagation – an example from Scotland. Geoderma 232–234 (November), 284–299.
Porcar-Castell, A., Tyystjärvi, E., Atherton, J., Van der Tol, C., Flexas, J., Pfündel, E.E., Moreno, J., Frankenberg, C., Berry, J.A., 2014. Linking chlorophyll a fluorescence to photosynthesis for remote sensing applications: mechanisms and challenges. J. Exp. Bot. 65 (15), 4065–4095.
Povey, A.C., Grainger, R.G., 2015. Known and unknown unknowns: uncertainty estimation in satellite remote sensing. Atmos. Meas. Tech. 8 (November (11)), 4699–4718.
Prévot, L., Chauki, H., Troufleau, D., Weiss, M., Baret, F., Brisson, N., 2003. Assimilating

optical and radar data into the STICS crop model for wheat. Agronomie 23 (4), 297–303.
Raffy, M., 1992. Change of scale in models of remote sensing: a general method for spatialization of models. Remote Sens. Environ. 40 (2), 101–112.
Revill, A., Sus, O., Barrett, B., Williams, M., 2013. Carbon cycling of European croplands: a framework for the assimilation of optical and microwave Earth observation data. Remote Sens. Environ. 137 (October), 84–93.
Ristic, B., Arulampalam, S., Gordon, N.J., 2004. Beyond the Kalman Filter: Particle Filters for Tracking Applications. Artech House.
Rosenzweig, C., Jones, J.W., Hatfield, J.L., Ruane, A.C., Boote, K.J., Thorburn, P., Antle, J.M., Nelson, G.C., Porter, C., Janssen, S., et al., 2013. The Agricultural Model Intercomparison and Improvement Project (AgMIP): protocols and pilot studies. Agric. For. Meteorol. 170, 166–182.
Rötter, R.P., Carter, T.R., Olesen, J.E., Porter, J.R., 2011. Crop-climate models need an overhaul. Nat. Clim. Change 1 (4), 175.
Ruane, A.C., Hudson, N.I., Asseng, S., Camarrano, D., Ewert, F., Martre, P., Boote, K.J., Thorburn, P.J., Aggarwal, P.K., Angulo, C., 2016. Multi-wheat-model ensemble responses to interannual climate variability. Environ. Model. Softw. 81 (C), 86–101.
Sasaki, Y., 1970. Some Basic Formalisms in Numerical Variational Analysis. Citeseer.
Schlee, F.H., Standish, C.J., Toda, N.F., 1967. Divergence in the Kalman filter. AIAA J. 5 (June (6)), 1114–1120.
Semenov, M.A., Doblas-Reyes, F.J., 2007. Utility of dynamical seasonal forecasts in predicting crop yield. Clim. Res. 34 (June), 71–81.
Shao, Y., Fan, X., Liu, H., Xiao, J., Ross, S., Brisco, B., Brown, R., Staples, G., 2001. Rice monitoring and production estimation using multitemporal RADARSAT. Remote Sens. Environ. 76 (3), 310–325.
Shen, S., Yang, S., Li, B., Tan, B., Li, Z., Le Toan, T., 2009. A scheme for regional rice yield estimation using ENVISAT ASAR data. Sci. China Ser. D: Earth Sci. 52 (8), 1183–1194.
Silvestro, P.C., Pignatti, S., Pascucci, S., Yang, H., Li, Z., Yang, G., Huang, W., Casa, R., 2017. Estimating wheat yield in China at the field and district scale from the assimilation of satellite data into the Aquacrop and simple algorithm for yield (SAFY) models. Remote Sens. 9 (5), 509.
Singh, G., Panda, R., 2015. Modelling and assimilation of root-zone soil moisture using near-surface observations from soil moisture ocean salinity (SMOS) satellite. In: ASABE 1st Climate Change Symposium: Adaptation and Mitigation Conference Proceedings. American Society of Agricultural and Biological Engineers. pp. 1.
Skakun, S., Vermote, E., Roger, J.-C., Franch, B., 2017. Combined use of Landsat-8 and Sentinel-2A images for winter crop mapping and winter wheat yield assessment at regional scale. AIMS Geosci. 3 (May (2)), 163–186.
Sus, O., Williams, M., Bernhofer, C., Béziat, P., Buchmann, N., Ceschia, E., Doherty, R., Eugster, W., Grünwald, T., Kutsch, W., Smith, P., Wattenbach, M., 2010. A linked carbon cycle and crop developmental model: description and evaluation against measurements of carbon fluxes and carbon stocks at several European agricultural sites. Agric. Ecosyst. Environ. 139 (November (3)), 402–418.
Swinbank, R., Kyouda, M., Buchanan, P., Froude, L., Hamill, T.M., Hewson, T.D., Keller, J.H., Matsueda, M., Methven, J., Pappenberger, F., et al., 2016. The TIGGE project and its achievements. Bull. Am. Meteorol. Soc. 97 (1), 49–67.
Talagrand, O., Courtier, P., 1987. Variational assimilation of meteorological observations with the adjoint vorticity equation. I: Theory. Q. J. R. Meteorol. Soc. 113 (478), 1311–1328.
Thorp, K., Wang, G., West, A., Moran, M., Bronson, K., White, J., Mon, J., 2012. Estimating crop biophysical properties from remote sensing data by inverting linked radiative transfer and ecophysiological models. Remote Sens. Environ. 124, 224–233.
Tian, L., Li, Z., Huang, J., Wang, L., Su, W., Zhang, C., Liu, J., 2013. Comparison of two optimization algorithms for estimating regional winter wheat yield by integrating MODIS leaf area index and world food studies model. Sens. Lett. 11 (6–7), 1261–1268.
Tian, Y., Woodcock, C.E., Wang, Y., Privette, J.L., Shabanov, N.V., Zhou, L., Zhang, Y., Buermann, W., Dong, J., Veikkanen, B., et al., 2002a. Multiscale analysis and validation of the MODIS LAI product: I. Uncertainty assessment. Remote Sens. Environ. 83 (3), 414–430.
Tian, Y., Woodcock, C.E., Wang, Y., Privette, J.L., Shabanov, N.V., Zhou, L., Zhang, Y., Buermann, W., Dong, J., Veikkanen, B., et al., 2002b. Multiscale analysis and validation of the MODIS LAI product: II. Sampling strategy. Remote Sens. Environ. 83 (3), 431–441.
Toan, T.L., Laur, H., Mougin, E., Lopes, A., 2017. Multitemporal and dual-polarization observations of agricultural vegetation covers by X-band SAR images. Eur. J. Nutr. 56 (3), 1339–1346.
Van der Linden, P., Mitchell, J.F.B.e., 2009. Ensembles: Climate Change and Its Impacts – Summary of Research and Results from the Ensembles Project.
Van Diepen, C.v., Wolf, J., Van Keulen, H., Rappoldt, C., 1989. WOFOST: a simulation model of crop production. Soil Use Manag. 5 (1), 16–24.
van Leeuwen, P.J., 2009. Particle filtering in geophysical systems. Mon. Weather Rev. 137 (12), 4089–4114.
van Leeuwen, P.J., 2010. Nonlinear data assimilation in geosciences: an extremely efficient particle filter. Q. J. R. Meteorol. Soc. 136 (October (653)), 1991–1999.
Van Oijen, M., Cameron, D., Butterbach-Bahl, K., Farahbakhshazad, N., Jansson, P.-E., Kiese, R., Rahn, K.-H., Werner, C., Yeluripati, J., 2011. A Bayesian framework for model calibration, comparison and analysis: application to four models for the biogeochemistry of a Norway spruce forest. Agric. For. Meteorol. 151 (12), 1609–1621.
Van Oijen, M., Rougier, J., Smith, R., 2005. Bayesian calibration of process-based forest models: bridging the gap between models and data. Tree Physiol. 25 (7), 915–927.
Vazifedoust, M., Van Dam, J., Bastiaanssen, W., Feddes, R., 2009. Assimilation of satellite data into agrohydrological models to improve crop yield forecasts. Int. J. Remote Sens. 30 (10), 2523–2545.
Vrugt, J.A., Gupta, H.V., Bouten, W., Sorooshian, S., 2003. A shuffled complex evolution metropolis algorithm for optimization and uncertainty assessment of hydrologic model parameters. Water Resour. Res. 39 (8).
Vrugt, J.A., Ter Braak, C.J., Clark, M.P., Hyman, J.M., Robinson, B.A., 2008. Treatment of input uncertainty in hydrologic modeling: doing hydrology backward with Markov chain Monte Carlo simulation. Water Resour. Res. 44 (12).
Wang, J., Li, X., Lu, L., Fang, F., 2013. Estimating near future regional corn yields by integrating multi-source observations into a crop growth model. Eur. J. Agron. 49, 126–140.
Wang, N., Wang, J., Wang, E., Yu, Q., Shi, Y., He, D., 2015. Increased uncertainty in simulated maize phenology with more frequent supra-optimal temperature under climate warming. Eur. J. Agron. 71, 19–33.
Weiss, M., Baret, F., Myneni, R., Pragnère, A., Knyazikhin, Y., 2000. Investigation of a model inversion technique to estimate canopy biophysical variables from spectral and directional reflectance data. Agronomie 20 (1), 3–22.
Weiss, M., Troufleau, D., Baret, F., Chauki, H., Prévot, L., Olioso, A., Bruguier, N., Brisson, N., 2001. Coupling canopy functioning and radiative transfer models for remote sensing data assimilation. Agric. For. Meteorol. 108 (June (2)), 113–128.
Wheeler, T., Challinor, A., Osborne, T., Slingo, J., 2007. Development of a combined crop and climate forecasting system for seasonal to decadal predictions. In: Sivakumar, M.V.K., Hansen, J. (Eds.), Climate Prediction and Agriculture: Advances and Challenges. Springer Berlin Heidelberg, Berlin, Heidelberg, pp. 31–40.
Whitcraft, A.K., Vermote, E.F., Becker-Reshef, I., Justice, C.O., 2015. Cloud cover throughout the agricultural growing season: impacts on passive optical earth observations. Remote Sens. Environ. 156, 438–447.
Williams, J., Jones, C., Kiniry, J., Spanel, D.A., 1989. The EPIC crop growth model. Trans. ASAE 32 (2), 497–511.
Wilson, A.M., Silander Jr., J.A., 2014. Estimating uncertainty in daily weather interpolations: a Bayesian framework for developing climate surfaces. Int. J. Climatol. 34 (June (8)), 2573–2584.
Wiseman, G., McNairn, H., Homayouni, S., Shang, J., 2014. RADARSAT-2 polarimetric SAR response to crop biomass for agricultural production monitoring. IEEE J. Sel. Top. Appl. Earth Obs. Remote Sens 7 (11), 4461–4471.
Wu, L., Liu, X., Wang, P., Zhou, B., Liu, M., Li, X., 2013. The assimilation of spectral sensing and the WOFOST model for the dynamic simulation of cadmium accumulation in rice tissues. Int. J. Appl. Earth Obs. Geoinf. 25, 66–75.
Wu, L., Liu, X., Zheng, X., Qin, Q., Ren, H., Sun, Y., 2015. Spatial scaling transformation modeling based on fractal theory for the leaf area index retrieved from remote sensing imagery. J. Appl. Remote Sens. 9 (1), 096015.
Wu, S., Huang, J., Liu, X., Fan, J., Ma, G., Zou, J., 2011. Assimilating MODIS-LAI into crop growth model with ENKF to predict regional crop yield. In: International Conference on Computer and Computing Technologies in Agriculture. Springer. pp. 410–418.
Wulder, M.A., Hilker, T., White, J.C., Coops, N.C., Masek, J.G., Pflugmacher, D., Crevier, Y., 2015. Virtual constellations for global terrestrial monitoring. Remote Sens. Environ. 170 (December), 62–76.
Xie, Y., Wang, P., Bai, X., Khan, J., Zhang, S., Li, L., Wang, L., 2017. Assimilation of the leaf area index and vegetation temperature condition index for winter wheat yield estimation using landsat imagery and the CERES-wheat model. Agric. For. Meteorol. 246, 194–206.
Xu, W., Jiang, H., Huang, J., 2011. Regional crop yield assessment by combination of a crop growth model and phenology information derived from MODIS. Sens. Lett. 9 (3), 981–989.
Yang, J., Reichert, P., Abbaspour, K.C., Xia, J., Yang, H., 2008. Comparing uncertainty analysis techniques for a SWAT application to the Chaohe Basin in China. J. Hydrol. 358 (1–2), 1–23.
Yang, K., Watanabe, T., Koike, T., Li, X., FUJII, H., Tamagawa, K., Ma, Y., Ishikawa, H., 2007. Auto-calibration system developed to assimilate AMSR-E data into a land surface model for estimating soil moisture and the surface energy budget. J. Meteorol. Soc. Jpn. Ser. II 85, 229–242.
Yang, W., Tan, B., Huang, D., Rautiainen, M., Shabanov, N.V., Wang, Y., Privette, J.L., Huemmrich, K.F., Fensholt, R., Sandholt, I., Weiss, M., Ahl, D.E., Gower, S.T., Nemani, R.R., Knyazikhin, Y., Myneni, R.B., 2006. MODIS leaf area index products: from validation to algorithm improvement. IEEE Trans. Geosci. Remote Sens. 44 (July (7)), 1885–1898.
Zhao, F., Li, R., Verhoef, W., Cogliati, S., Liu, X., Huang, Y., Guo, Y., Huang, J., 2018. Reconstruction of the full spectrum of solar-induced chlorophyll fluorescence: intercomparison study for a novel method. Remote Sens. Environ. 219, 233–246.
Zhu, Y., Zhu, Y., Huang, Y., Yao, X., Liu, L., Cao, W., Tian, Y., 2010. Assimilation technique of remote sensing information and rice growth model based on particle swarm optimization. Yaogan Xuebao – J. Remote Sens. 14 (6), 1226–1240.
Ziehn, T., Scholze, M., Knorr, W., 2012. On the capability of Monte Carlo and adjoint inversion techniques to derive posterior parameter uncertainties in terrestrial ecosystem models. Glob. Biogeochem. Cycles 26 (September (3)), GB3025.
Zupanski, D., 1997. A general weak constraint applicable to operational 4DVAR data assimilation systems. Mon. Weather Rev. 125 (9), 2274–2292.